Static and dynamical properties of doped Hubbard clusters

E. Dagotto, A. Moreo, F. Ortolani,* D. Poilblanc,† and J. Riera‡
Department of Physics and Center for Materials Research and Technology, Florida State University, Tallahassee, Florida 32306
(Received 25 July 1991; revised manuscript received 12 November 1991)

We study the *t-J* and the Hubbard models at zero temperature using exact-diagonalization techniques on $\sqrt{10}\times\sqrt{10}$ and 4×4 sites clusters. Quantum Monte Carlo simulation results on larger lattices are also presented. All electronic fillings have been analyzed for the three models. We have measured equal-time correlation functions corresponding to various types of order (ranging from "standard" staggered spin order to more "exotic" possibilities like chiral order), as well as various dynamical properties of these models. Upper bounds for the *critical hole doping* (x_c), where long-range antiferromagnetic order disappears, are presented. It was found that x_c is very small in agreement with experiments for the high-T_c superconductors. For example, in the *t-J* model, $x_c<0.08$ at $J/t=0.4$. However, short-distance spin correlations are important up to much higher dopings producing a sharp well-defined spin-wave-like peak in $S(\mathbf{q}=(\pi,\pi),\omega)$. Regarding the possibility of *phase separation* in the Hubbard model, we have studied the behavior of the density of particles, $\langle n\rangle$, as a function of the chemical potential, using the Lanczos method on a 4×4 Hubbard cluster, finding no indications of phase separation for any value of U/t. Then, we conclude that the *t-J* model at small J/t should *not* phase separate. In order to compare theoretical predictions with photoemission experiments, we evaluated the *electronic density of states*, $N(\omega)$, of the Hubbard and *t-J* models at several doping fractions. We found that upon doping the antiferromagnetic gap is filled for $U\sim8t$ or smaller. The chemical potential moves across the insulating gap as one goes from electron to hole doping of the half-filled cluster, in agreement with x-ray absorption experiments but at variance with photoemission experiments. We have also calculated the *optical conductivity*, $\sigma_1(\omega)$, of the Hubbard and *t-J* models at all dopings on 4×4 clusters. Results are compared with experiments and the weight of the Drude peak is presented as a function of couplings and dopings. Spectral weight found at small frequencies is associated with the mid-infrared band observed experimentally in $La_{2-x}Sr_xCuO_4$, and with the states filling the insulating gap in photoemission experiments. An overall good agreement with experiments in the normal state was found. Regarding the possibility of *superconductivity* in these models, we have studied *s*-, *d*-, and *p*-wave pairing correlations. Naively, the *d*-wave channel seems enhanced near half filling while the extended *s*-wave channel seems enhanced from half filling up to 40% doping. However, we found that the enhancement comes from *short-distance* effects and, thus, *no* numerical indications of superconductivity were found in these models. We emphasize the importance of analyzing the pairing correlations as a function of distance to distinguish between short- and long-distance effects in the susceptibilities. We also observed that *spiral* order is enhanced at small J/t and low doping. *Uniform chiral* order is suppressed by dynamical holes while *staggered chiral* order may be enhanced, although with a small plaquette order parameter. We conclude with the observation that the simple one-band Hubbard model with intermediate values of $U\sim8t$ may account for many of the "anomalous" properties of the normal state of the high-T_c superconductors.

I. INTRODUCTION

It is widely agreed that the insulating antiferromagnetic state of the high-temperature superconducting Cu-O materials[1] is characterized by a charge-transfer (CT) gap[2] of about 1.5–2.0 eV while the nature of the "normal" state (above the superconducting critical temperature) which arises from the doping of the insulating state still remains a puzzle. Many of the normal-state properties of these superconducting materials have been labeled as "anomalous." Although the gap at half filling is not of the Mott-Hubbard type but of charge-transfer origin, a one-band Hubbard model may still qualitatively describe the materials once the valence band, which has mainly O $2p$ character, is identified with the lower Hubbard band while the Cu $3d$ conduction band is associated with the upper Hubbard band. An *effective* coupling U/t can be found that approximately reproduces the spectrum of a more involved Cu-O Hamiltonian.[3] For this reason, the two-dimensional Hubbard and *t-J* modes have recently attracted considerable attention as simple phenomenological models for the description of the CuO_2 planes of high-temperature superconductors like $La_{2-x}Sr_xCuO_4$. At half filling, these superconducting cuprates are insulating and they present staggered spin order, facts well reproduced by these models. It is particularly important to understand the evolution of the ground state at half filling (which has staggered spin order) when the system is doped with holes or electrons. Many mean-field and Hartree-Fock calculations have appeared in the literature discussing different "standard" and "exotic" phases. However, these approaches, which are intrinsically varia-

tional, cannot properly analyze the *global* stability of the proposed mean-field solutions since it is difficult in a single calculation to compare free energies of all the possible ground states. In addition, and specially at large couplings, the many-body effects seem crucial to understand the behavior of strongly correlated electronic systems. Then, numerical results like those presented in this paper, are very important to clarify the properties of these models in the intermediate- and large-(U/t) regions.

The one-band Hubbard model is defined by the Hamiltonian

$$H=-t\sum_{\langle ij\rangle,s}(c^{\dagger}_{i,s}c_{j,s}+\text{H.c.})+U\sum_{i}n_{i\uparrow}n_{i\downarrow}\ , \tag{1}$$

where $c^{\dagger}_{i,s}$ is an operator that creates an electron at site i of a two-dimensional (2D) lattice with periodic boundary conditions and N sites. s denotes spin, $\langle ij\rangle$ represents nearest-neighbors sites, and n_i is the number operator. The t-J model corresponds to the strong-coupling limit of the Hubbard model and is defined by the Hamiltonian

$$H=J\sum_{\langle ij\rangle}(\mathbf{S}_i\cdot\mathbf{S}_j-\tfrac{1}{4}n_in_j)-t\sum_{\langle ij\rangle,s}(\bar{c}^{\dagger}_{i,s}\bar{c}_{j,s}+\text{H.c.})\ , \tag{2}$$

where J is the exchange constant of the spin-spin interaction and t corresponds to the hopping parameter of the kinetic energy of holes. $\bar{c}_{i,s}$ are *hole* operators and $\mathbf{S}_i=\frac{1}{2}c^{\dagger}_i\sigma c_i$. There is no double occupancy in this model. It has been suggested that the t-J model may be more fundamental than the Hubbard model since (under some approximations) it can be derived from a general Cu-O Hamiltonian and thus it should be independently analyzed.[4]

How can we extract useful information from these Hamiltonians? In the absence of exact results, the most reliable way to describe the actual ground-state properties of strongly correlated models are numerical techniques. Regretfully, these methods also have limitations. For example, quantum Monte Carlo (QMC) techniques at finite doping have the complication of negative fermionic determinants and finite temperature effects. A technique that avoids this problem is the exact diagonalization of small clusters using the Lanczos method. Actually, with this procedure interesting information has been produced about dynamical properties of the t-J model, frustrated models, and other systems where there are no efficient Monte Carlo methods available.[5] Of course, the main limitation of the Lanczos technique is the constraint of working on small clusters due to the rapid increase in the size of the Hilbert space with the number of sites.

In this paper, we present a numerical study of *static* and *dynamical* correlation functions of the 2D Hubbard and t-J models at *all* doping fractions using lattices of up to 4×4 sites. For both models, such an analysis was possible after a major computational effort due to the large size of their Hilbert spaces. Many different types of correlations were calculated including those corresponding to superconductivity. We also compare our predictions for the electronic spectral function and the optical conductivity with experiments finding an overall encouraging qualitative agreement.

The organization of the paper is as follows. In Sec. II, we briefly review some of the features of the numerical technique used in the paper. Section III contains the quantum numbers of the ground state of these models as a function of doping and couplings. In Sec. IV we start comparing theoretical predictions with experiments. The section is devoted to the analysis of antiferromagnetic order and its evolution as a function of doping. In Sec. V we discuss the issue of phase separation as well as the behavior of the chemical potential with doping. Section VI is devoted to the analysis of the electronic spectral density, $N(\omega)$, contrasting our results with those of x-ray absorption and photoemission experiments. In Sec. VII the optical conductivity, $\sigma_1(\omega)$, is evaluated and compared with experiments. Section VIII reports on attempts to search for superconductivity in these models while in Secs. IX and X we analyze the possible existence of flux, chiral, or spiral order at finite doping. Our conclusions are presented in Sec. XI.

II. NUMERICAL TECHNIQUE

The numerical technique that we will mainly use is the Lanczos method that allows us to obtain exact results for the Hubbard and t-J models on small clusters at zero temperature. We also present additional data using the quantum Monte Carlo method. With these techniques some preliminary results for the Hubbard and t-J models have been previously discussed, finding good qualitative agreement between theory and experiment at low doping[5] in the normal state. Below, we present results for *equal*-time correlation functions of different order parameters (as well as spectral functions) of various operators related with possible different phases of these models. We also present *dynamical* correlation functions which are difficult to obtain using other numerical methods.[6] We were able to study different values of the couplings U/t and J/t, since our technique works equally well at strong and weak coupling. We were also able to analyze all possible doping fractions on the 4×4 and $\sqrt{10}\times\sqrt{10}$ clusters since using Lanczos algorithm we do not have "sign" problems as in a QMC simulation. However, the study of the 4×4 Hubbard model is still a difficult task since its Hilbert space is very large. In order to reduce the size of the matrices to be diagonalized we have explicitly exploited various symmetries of the model, i.e., conservation of the number of particles, conservation of the projection along the z axis of the total spin, as well as invariance under translations, rotations, reflexions, and spin inversion. At half filling, the largest subspace we have studied contains $\sim 1\,350\,000$ states.[7]

The study of the t-J model on a 4×4 cluster is also a difficult task. For this cluster most of the work previously reported in the literature was performed with 0, 1, and 2 holes. The reason is that the size of the Hilbert space grows with the number of holes reaching a maximum at a doping fraction $\frac{5}{16}$ where the dimension of the matrices we studied numerically is of $\sim 126\,000$ states even after the many symmetries discussed above were implemented. A study for *all* possible dopings of different correlation functions in the 2D Hubbard and t-J models has not been previously attempted to the best of our knowledge. All

these calculations have been performed on a Cray-2 supercomputer.

III. QUANTUM NUMBERS OF THE GROUND STATE

In this section we present the quantum numbers of the ground state of the Hubbard and t-J models as a function of doping for the 4×4 cluster. We report on the momentum $\mathbf{k}$, the quantum number under a $\pi/2$ rotation (s, d, or p waves) for an *even* number of particles and, only for the t-J model, the total spin S. In the case of the t-J model, the results presented below have been obtained for values of the coupling J/t between 0.1 and 2 while for the Hubbard model we work with U/t between 4 and 20. The reason is the following: As previously discussed in the case of one hole,[8] for $J/t>2.0$ there are many crossing of levels in the ground state[9] and its quantum numbers are tedious to describe (although they can be understood[8] by perturbation theory in t/J). Since large J/t is not the most interesting physical regime, we will not provide in this paper information about level crossings in that region. A similar situation occurs in the other extreme of very small J/t. As was also discussed for the case of one hole,[8] finite-size effects for a 4×4 lattice are certainly important for $J/t<0.1$ and thus it is not clear whether these additional level crossings will survive the bulk limit. The physical reason for this problem is that when J/t is decreased, the hole (thought of as a polaron) increases its "size" until it reaches the boundary of the 4×4 clusters. Thus, below we present the quantum numbers of the t-J model only in the intermediate region of parameters $J\in[0.1,2.0]$. We follow a similar procedure or the Hubbard model. In weak coupling (small U/t) it is well known that finite-size effects are important, since correlation lengths are large. In the other limit of very large U/t, there are many level crossings similar to those of the t-J model for small J/t. Then, as before, we restrict our analysis to the region $U\in[4,20]$ that contains the phenomenologically important[3] values of the coupling U/t.

Unless otherwise stated, the quantum numbers presented below for various doping fractions are valid for *both* the Hubbard and t-J model. The hopping t is taken equal to 1. Periodic boundary conditions were used. Degeneracies due to rotations of the lattice in $\pi/2$ are not made explicit. However, degeneracies produced by the special shape of the 4×4 cluster (which is equivalent to a 2^4 hypercube[8]) are carefully discused for the t-J model.

0 holes: $\mathbf{k}=(0,0)$, $S=0$, s wave.

1 hole: $\mathbf{k}=(\pi/2,\pi/2)$ [degenerate with $\mathbf{k}=(0,\pi)$], $S=\frac{1}{2}$.

2 holes: $\mathbf{k}=(0,0)$ [degenerate with $\mathbf{k}=(0,\pi)$], $S=0$, d wave.

3 holes: For $J\in[0.4,2.0]$, $S=\frac{1}{2}$ with $\mathbf{k}=(\pi/2,\pi/2)$ [degenerate with (π,π)]. For $J=0.2$, $S=\frac{3}{2}$, $\mathbf{k}=(0,0)$ [degenerate with $(0,\pi)$]. For $J=0.1$, $S=\frac{5}{2}$, $\mathbf{k}=(\pi,\pi)$ [degenerate with $(\pi/2,\pi/2)$]. For $U\in[4,10]$, $S=\frac{1}{2}$ with $\mathbf{k}=(\pi/2,\pi/2)$ [degenerate with (π,π)].

4 holes: For $J\in[0.4,2.0]$, $\mathbf{k}=(0,0)$ [degenerate with $\mathbf{k}=(0,\pi)$], $S=0$, d wave. For $J=0.2$ and 0.1, $\mathbf{k}=(0,0)$ [degenerate with (π,π)], $S=0$, s wave. For $U\in[8,20]$, $\mathbf{k}=(0,0)$, $S=0$, s wave, while at $U=4$, $\mathbf{k}=(0,0)$, $S=0$ but d wave.

5 holes: $\mathbf{k}=(\pi/2,\pi/2)$ [degenerate with $\mathbf{k}=(0,\pi)$], $S=\frac{1}{2}$.

6 holes: $\mathbf{k}=(0,0)$, $S=0$, s wave.

7 holes: $\mathbf{k}=(0,\pi/2)$, $S=\frac{1}{2}$.

8 holes: $\mathbf{k}=(0,0)$ [degenerate with $\mathbf{k}=(0,\pi)$], $S=0$, d wave.

9 holes: For $J\in[0.6,2.0]$, $\mathbf{k}=(0,\pi/2)$ [degenerate with $\mathbf{k}=(\pi,\pi/2)$], $S=\frac{1}{2}$. For $J=0.4$ or smaller $\mathbf{k}=(0,\pi/2)$ with $S=\frac{3}{2}$. For the Hubbard model $\mathbf{k}=(0,\pi/2)$.

10 holes: For $J\in[0.8,2.0]$, $\mathbf{k}=(0,0)$ [degenerate with $\mathbf{k}=(\pi,\pi)$], $S=0$, s wave. For $J=0.6$ or smaller $\mathbf{k}=(0,0)$, $S=2$. For the Hubbard model $\mathbf{k}=(0,0)$ and it is odd under *both* a reflection along the x or y axis.[10]

11 holes: For $J\in[0.8,2.0]$, $\mathbf{k}=(0,\pi/2)$ [degenerate with $\mathbf{k}=(\pi,\pi/2)$]. For $J=0.6$ or smaller, $\mathbf{k}=(0,\pi/2)$, $S=\frac{3}{2}$. For the Hubbard model $\mathbf{k}=(0,\pi/2)$.

12 holes: $\mathbf{k}=(0,0)$ [degenerate with $\mathbf{k}=(0,\pi)$], $S=0$, d wave.

13 holes: $\mathbf{k}=(0,\pi/2)$, $S=\frac{1}{2}$.

14 holes: $\mathbf{k}=(0,0)$, $S=0$, s wave.

Many features of these quantum numbers are important to discern.

(i) There exists a region where the ground state with an even number of particles is *s wave*. This occurs at dopings of $x=0.25$ and $x=0.37$ in both models (four and six holes, respectively). Closer to half filling the ground state is a d wave. This issue will be discussed later in Sec. VIII and is related with the possibility of s-wave superconductivity in these models.[11]

(ii) Both models have very similar quantum numbers. This gives support to the idea that the physics of the Hubbard model at large coupling is well described by the t-J model for small J/t. It also shows that there is a smooth connection between the strong- and weak-coupling regions of the Hubbard model and no singularities are found between those two regimes.

(iii) At large hole doping (small density of electrons), the quantum numbers are in good agreement with a picture of noninteracting particles for both models.

IV. INFLUENCE OF DOPING ON ANTIFERROMAGNETIC ORDER

We start our comparison of theoretical predictions for Hubbard-like models in 2D with experiments for the high-T_c cuprates, by analyzing their magnetic properties. It is particularly interesting to study the evolution of the antiferromagnetic (AF) order present at half filling, when the Hubbard and t-J models are doped by holes or electrons. In the high-T_c superconductors AF order is rapidly suppressed by doping. For example, in $La_{2-x}Sr_xCuO_4$ the Néel temperature is reduced[12] from 300 K at half filling to below 10 K for a doping fraction $x\sim0.02$, while for the electron-doped material $Nd_{2-x}Ce_xCuO_{4-y}$ the antiferromagnetic order disappears[13] at an electronic doping $x\sim0.14$

Can this effect be reproduced by the strongly correlat-

ed models we are analyzing? To study this question we have calculated various quantities with spin order. Consider the spectral decomposition of the operator that creates spin waves with momentum $\mathbf{q}$, i.e., $S_{\mathbf{q}}^{+}=(1/\sqrt{N})\sum_{j}e^{i\mathbf{q}\cdot\mathbf{j}}c_{j,\uparrow}^{\dagger}c_{j,\downarrow}$ in the t-J model. Its spectral function can be written as

$$S(\mathbf{q},\omega)=\sum_{n}|\langle n|S_{\mathbf{q}}^{+}|0\rangle|^{2}(\omega-(E_{n}-E_{0}))\ , \tag{3}$$

where $\{|n\rangle\}$ are states connected to the ground state by the action of $S_{\mathbf{q}}^{+}$ and $\{E_n\}$ are their energies. If the ground state is a singlet with zero momentum, then the states $\{|n\rangle\}$ are triplets with momentum $\mathbf{q}$. $|0\rangle$ is the ground state of the model at the corresponding values of doping and coupling under consideration and E_0 is its energy. In Fig. 1(a)–1(d) we show $S(\mathbf{Q},\omega)$ [$\mathbf{Q}=(\pi,\pi)$] for the t-J model at $J=0.4$ ($t=1$ in the rest of the paper unless otherwise stated) and various doping fractions. The momentum $\mathbf{q}=\mathbf{Q}$ corresponds to the spin-wave excitation of lowest energy at half filling (due to the staggered spin antiferromagnetic order). In Fig. 1 we observed that up to a doping fraction $x\sim0.25$ there is a sharp peak at the bottom of the spectrum and the spin-wave excitation is well defined. Increasing the doping further to $x\sim0.37$, the peak is still well defined but its energy is higher (and, thus, a clear and large spin gap develops). Finally, at quarter filling $x\sim0.50$, the spectrum is already *incoherent* and there is no well-defined peak associated with spin waves of that momentum. This behavior is qualitatively similar to that recently reported[14] for $YBa_2Cu_3O_{6+x}$, where it was found that spectral weight of the magnetic scattering shifts to higher energies as the oxygen concentration increases.

Naively, Fig. 1 would suggest that long-range antiferromagnetic order is lost between $x=0.25$ and $x=0.37$, which are dopings too large compared with experiments. However, short-distance staggered fluctuations may still induce large well-defined peaks in the spectrum even without a genuine long-range order and thus the actual critical doping may be much smaller. To clarify this issue we have studied the (spin) energy gaps between the ground state of the t-J model (at different doping fractions) and the first excited state that appears in the spectral decomposition Eq. (3) when a spin wave of a given momentum is created.[15] The results are shown in Figs. 2(a) and 2(b) at $J=0.4$ and 1.0. We observe that near half filling ($x=0$) the first excited state has momentum $\mathbf{q}=(\pi,\pi)$ (as expected from the existence of antiferromagnetic long-range order) and it is well separated from the rest of the spectrum. This state will become the massless (zero-energy gap) spin-wave state in the bulk limit at half filling. However, note that for a doping of only two holes (roughly $x\sim0.125$) most of the spin-wave states with different momenta have a comparable energy. Moreover, for a doping of four holes ($x=0.25$) the lowest-energy state has $\mathbf{q}=(\pi/2,\pi/2)$ rather than $\mathbf{q}=(\pi,\pi)$. This result suggests that AF order is lost faster than what the spectral decomposition (Fig. 1) would imply.[16]

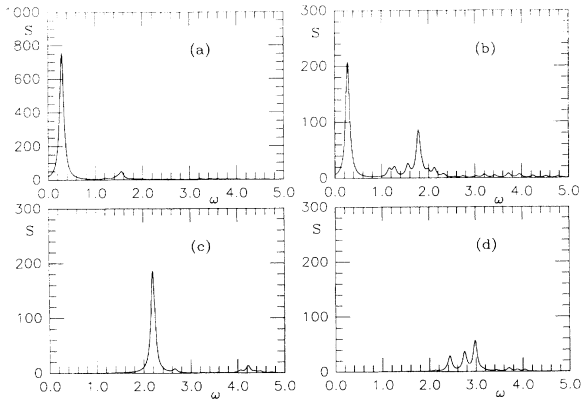

FIG. 1. $S=S(\mathbf{Q},\omega)$ [$\mathbf{Q}=(\pi,\pi)$] as a function of ω at $J=0.4$ for different doping fractions and a 4×4 cluster: (a) $x=0.125$, (b) $x=0.25$, (c) $x=0.375$, (d) $x=0.50$. The units in the vertical axis are arbitrary.

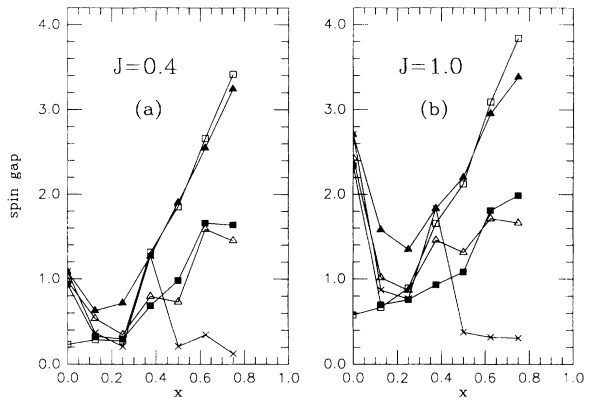

FIG. 2. Spin gap (defined as the difference in energy between the first excited state created by $S_{\mathbf{q}}^{+}$ and the ground state) as a function of doping for different momenta: open squares denote $\mathbf{q}=(\pi,\pi)$; full squares $\mathbf{q}=(\pi,\pi/2)$; open triangles are $\mathbf{q}=(0,\pi/2)$; full triangles have $\mathbf{q}=(0,\pi)$; and crosses denote $\mathbf{q}=(\pi/2,\pi/2)$. (a) is at $J=0.4$ and (b) at $J=1.0$.

In Fig. 3 we show the equal-time staggered spin-spin correlation function defined as

$$C(\mathbf{i})=4\langle S_{\mathbf{i}}^{z}S_{0}^{z}\rangle(-1)^{i_x+i_y}\ , \tag{4}$$

as a function of doping for various distances ($\mathbf{i}=(i_x,i_y)$, $|\mathbf{i}|=\sqrt{i_x^2+i_y^2}$). In principle, in our small 4×4 lattice there is not enough space to make a proper study of the decay of correlation functions with distance. However, we can still analyze for what values of dopings and couplings the antiferromagnetic correlations at the distances allowed in our cluster change sign (suggesting the absence of long-range staggered order). In Fig. 3(c) we find that the correlation at the maximum possible distance on the 4×4 lattice, i.e., $2\sqrt{2}$ lattice spacings, changes sign at $x\sim0.20$ for $J=1.0$ and at smaller dopings when J is reduced. Working on larger lattices and for distances larger than $2\sqrt{2}$, it is reasonable to expect that the value of x where the correlations change sign would be even smaller. On the other hand, the staggered spin correlations at very short distances remain important up to

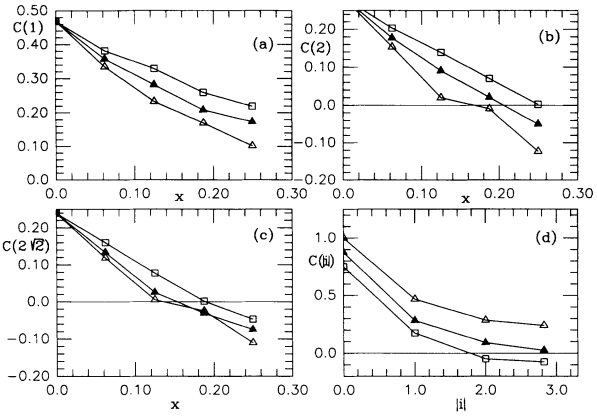

FIG. 3. Equal-time spin-spin correlation functions $C(i)$ [Eq. (4)] on a 4×4 cluster at distances: (a) $|\mathbf{i}|=1$; (b) $|\mathbf{i}|=2$; (c) $|\mathbf{i}|=2\sqrt{2}$ for $J=0.2$ (open triangles), $J=0.4$ (full triangles), and $J=1.0$ (open squares) as a function of doping. The actual dependence of $C(\mathbf{i})$ with distance for $x=0.0$ (open triangles); $x=0.125$ (full triangles); and $x=0.25$ (open squares); all at $J/t=0.4$, is shown in (d).

higher dopings [Figs. 3(a) and 3(b)]. For example, for nearest-neighbor spins, Fig. 3(a), there is no change of sign even at the relatively large doping of $x\sim 0.25$ for *any* value of J. This result is compatible with Fig. 1 where a sharp peak appears in the spectral decomposition up to large doping fractions. We believe that the peak is created by short-distance fluctuations rather than by long-range order (LRO). As stated before, it is possible to find upper bounds on the critical dopings necessary to destroy AF order in the t-J model by analyzing at what doping the correlation functions of, e.g., Fig. 3(c) change sign. For example, at $J=1.0$ we find $x_c<0.20$; at $J=0.4$, $x_c<0.15$ and at $J=0.2$, $x_c<0.12$, approximately. These bounds on x_c are better than those obtained by analyzing the spectral function (Fig. 1) or the correlation functions at zero momentum.[17] Exploratory studies for the Hubbard model in strong coupling on a 4×4 cluster suggest results similar to those of the t-J model. Finally, the explicit dependence of the spin-spin correlation function with doping is presented in Fig. 3(d) for various filling fractions at $J=0.4$.

The existence of a very small x_c for the t-J model is in agreement with the following simple scenario. Suppose that the holes are uniformly spread on the square lattice. Each hole in its ground state is surrounded by a region where antiferromagnetism is depleted.[18] This region is larger than just one site and it is produced by the competition between the kinetic energy of the hole (which is minimized increasing the "size" of the hole) against the exchange energy (which tries to maximize the number of antiferromagnetically aligned spins and thus reduces the size of the hole).[19] In previous studies of one hole in the t-J model it was found[8] that a hole injected in an antiferromagnetic background is well described by a Schrödinger equation in a linear potential[20] (this potential being caused by the "strings" created by the hole in its movement). The "size" (d) of the one-hole ground state in this linear potential depends on J (at $t=1$) as $d\approx 1.43/J^{0.33}$, which corresponds to approximately two lattice spacings at $J=0.4$. On a disk of radius $r=2$ there are ~ 13 spins. Then, roughly, for a doping of $x_c=\frac{1}{13}=0.08$ every spin of the lattice belongs to a certain "spin bag" and LRO is lost. In general,

$$x_c=J^{0.66}/[\pi(1.43)^2]\approx 0.16J^{0.66}\ , \tag{5}$$

which gives a critical doping fraction of $x_c=0.16$, 0.08, and 0.05 at $J=1.0$, 0.4, and 0.2, respectively, in qualitative agreement with the upper bounds quoted above from Fig. 3(c).

Then, studying the staggered spin order in the t-J model we found that indeed the critical doping where AF disappears is very *small*, which is compatible with experimental results. The main intuitive explanation for this effect is that "dressed" holes in a spin background are *larger* than just one lattice spacing. Actually their size diverges as $J\to 0$. Thus, it is not surprising that a very small doping fraction is able to completely destroy the antiferromagnetic LRO and the Hubbard and t-J models can neatly explain this phenomenon.[21]

V. PHASE SEPARATION IN STRONGLY CORRELATED SYSTEMS

At very large J/t and nonzero doping, it is well known that the t-J model phase separates. This occurs because the configuration of minimum energy is obtained when the number of "broken" or missing antiferromagnetic links is minimized. Suppose that the system is initially prepared in a state with a given hole doping fraction x. This state will evolve in time such that the holes will tend to "cluster" into a giant nucleus, leaving the rest of the system undoped. Then, the original doping fraction x does not correspond to a thermodynamically stable state. The equilibrium configuration consists of two separated regions with different hole densities.[22] Phase separation may compete with superconductivity since both are induced by energetic attraction of pairs of holes. Thus, it is important to know to what extent this effect dominates in the t-J model. Recently, it has been suggested[23] that phase separation occurs in this model for *all* values of J/t. On the other hand, quantum Monte Carlo simulations at finite temperature[24] of the Hubbard model have *not* found indications of phase separation. These results seem contradictory since both models should show similar behavior in the large-(U/t) region.

In this section we study phase separation in the Hubbard and t-J models using exact diagonalization techniques on a 4×4 cluster at zero temperature. A simple way to study this problem is by monitoring the average number of particles $\langle n\rangle$ per site as a function of the chemical potential μ of the system.[24] If there is a discontinuity in $\langle n\rangle$ vs μ, at some particular value of the chemical potential μ^*, it means that the densities inside the gap in $\langle n\rangle$ are not stable. If a system is initially prepared with these densities, it will phase separate. On a finite system with N sites, the possible densities below half filling are given by $(N-N_h)/N$ where N_h is the number of holes (defined as the number of sites N minus the number of electrons) that can take values ranging be-

tween 0 and N. If the calculated density $\langle n \rangle$ changes by steps of $1/N$ as a function of the chemical potential, then there is neither pairing nor phase separation. If the change is given by $2/N$, then we will say that there is "pairing" of holes. These pairs may Bose condense leading to a superconducting state. Finally, if the change in the density is larger than $2/N$, we say that the system phase separates.

We calculate the curve $\langle n \rangle$ vs μ for a finite system at zero temperature in the following way: Using a Lanczos algorithm we obtain the lowest-energy eigenvalues E_h at all possible fillings N_h, for particular values of the couplings J/t or U/t. These results are obtained at zero chemical potential using Hamiltonians Eqs. (1) and (2). Adding a chemical potential will modify the energy levels by $-\mu N_h$. When $\mu=0$ the energy of the t-J and Hubbard Hamiltonians as written in Eqs. (1) and (2) is minimized by a finite number of holes. Thus, in order to make stable a half-filled ground state we need to introduce a negative chemical potential to the Hamiltonian. Adding a term $-(U/2)\hat{N}+(U/4)N$ to the Hubbard model (where $\hat{N}$ is the number operator), makes the Coulombic interaction explicitly particle-hole symmetric, i.e., the new Hamiltonian is

$$H=-t\sum_{\langle ij\rangle,s}(c^{\dagger}_{is}c_{js}+c^{\dagger}_{js}c_{is})+U\sum_{i}(n_{i\uparrow}-\tfrac{1}{2})(n_{i\downarrow}-\tfrac{1}{2}) -\mu\sum_{i,s}(n_{is}-\tfrac{1}{2}) . \quad (6)$$

Now, for $\mu=0$ the ground-state density is $\langle n \rangle=1$ as expected. Recalling that $J=4t^2/U$, we add a similar term $(t^2/J)(N-2\hat{N})$ to the t-J model. This is the convention that we have followed in the present paper.

The particular values of μ that correspond to a change in the density are obtained in the following way starting at half filling. When $E_h-\mu N_h=E_0$, the ground state in the subspace with N_h holes crosses the half-filled ground state whose energy is E_0. This, obviously, occurs at a value of μ that satisfies

$$\mu(N_h)=(E_h-E_0)/N_h . \quad (7)$$

The level that first crosses E_0, i.e., for the smallest value of μ, is the one that becomes the new ground state. Thus, we have to calculate the minimum μ [Eq. (7)] as a function of N_h. Suppose that the state that crosses E_0 for the smallest μ has $N_h=2$. Then, in this particular case a state with $N_h=1$ *cannot* become the ground state and we say that the system has "pairing" of holes. If, on the other hand, the next stable state after half filling has N_h larger than 2, this means that all the states with a number of holes smaller than this N_h cannot be the ground state of the system and this is what we call phase separation. This is completely equivalent to the Maxwell construction presented by Emery, Kivelson, and Lin[23] that allows the study of phase separation between the half-filled and a doped state. They find the minimum in $(E_h-E_0)/N_h$ as a function of N_h and if this minimum is obtained for any $N_h>1$, they claim that there is a phase separation (they include our definition of pairing in their definition of phase separation).

The evaluation of the whole curve $\langle n \rangle$ vs μ allows us to look for the possibility of phase separation even away from half filling. We proceed in the following way. If E_H is the energy at $\mu=0$ of a state with N_H holes that becomes the ground state at some value of $\mu=\mu_H$, we can find at what value of μ this state is itself replaced as ground state and the doping of the new state. This is done by solving the following equation:

$$\mu=(E_h-E_H)/(N_H-N_h) , \quad (8)$$

for all values of N_h larger than N_H, and obtaining the minimum μ with respect to N_h. The Maxwell construction can also be applied to the study of phase separation away from half filling. It can be restated in the following way: If the curve ground-state energy vs $\langle n \rangle$ has negative curvature between two different values of $\langle n \rangle$, then phase separation occurs between these two densities.

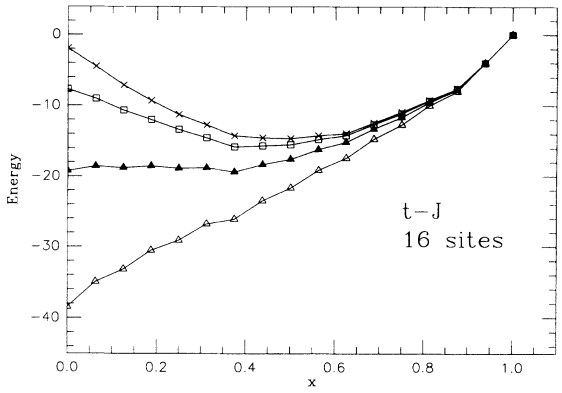

FIG. 4. Energy of the ground state of the t-J model on a 4×4 lattice for $J=0.2$ (crosses); $J=0.4$ (open squares); $J=1.0$ (full triangles); $J=2.0$ (open triangles).

In Fig. 4 we show the energy of the ground state of the t-J model on a 4×4 lattice as a function of $x=N_h/N$ for many values of J/t. The actual values of the energy are presented in Table I. For $J/t=2.0$ the curvature is slightly negative between $x=1$ and $x=\frac{6}{16}$ indicating that there is phase separation into two regions with these two densities. Increasing further J/t the region of negative curvature is even larger. On the other hand, for $J/t=0.4$ and 0.2 the curvature is negative only close to half filling ($x=0$) between neighboring densities indicating pairing but not phase separation. This is in agreement with previous studies of hole binding in this model,[25] which showed that phase separation only starts at $J/t>0.6$ at least on a 4×4 lattice while in the interval $0.2<J/t<0.6$ there is hole binding (pairing).

In Fig. 5 we present the density as a function of the chemical potential for the t-J model (after shifting appropriately μ such that $\langle n \rangle=1$ for $\mu=0$). At $J/t=0.4$, there are no sharp discontinuities in the results. Close to half filling the ground states with two, four, and six holes are stable (they "exist" by appropriately tuning μ) while the states with one, three, and five holes are unstable (no matter what value μ takes, they never become the ground state of the system). This means that there is "binding of holes" in this region but *not* phase separation. On the other hand, for $J/t=1.0$ and 2.0 the state with $\langle n \rangle=\frac{10}{16}$

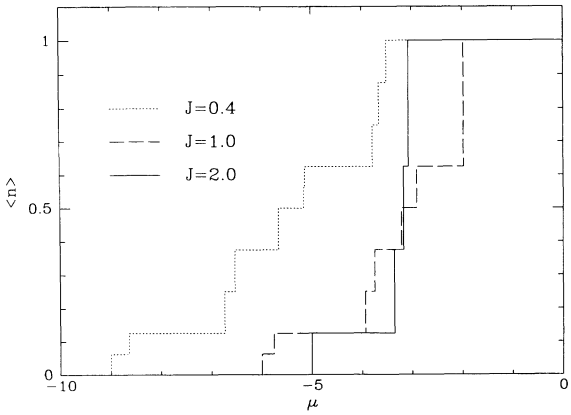

FIG. 5. Density $\langle n \rangle$ vs μ for the t-J model on a 4×4 cluster at different values of J ($t=1$).

is the first stable one after half filling. The curve $\langle n \rangle$ vs μ has a discontinuity of $\Delta\langle n \rangle = 0.375$ indicating the existence of phase separation. Increasing J/t the jump in the density also increases. At $J/t=10$, it is already at its saturation value $\Delta\langle n \rangle = 1$.

Now let us contrast our results for the t-J model with those for the Hubbard model. In Fig. 6 we show exact results for the ground-state energy of the Hubbard model Eq. (6) at $\mu=0$ on $\sqrt{10}\times\sqrt{10}$ and 4×4 lattices for various values of U/t ranging from intermediate to strong couplings. The actual values of the ground-state energies

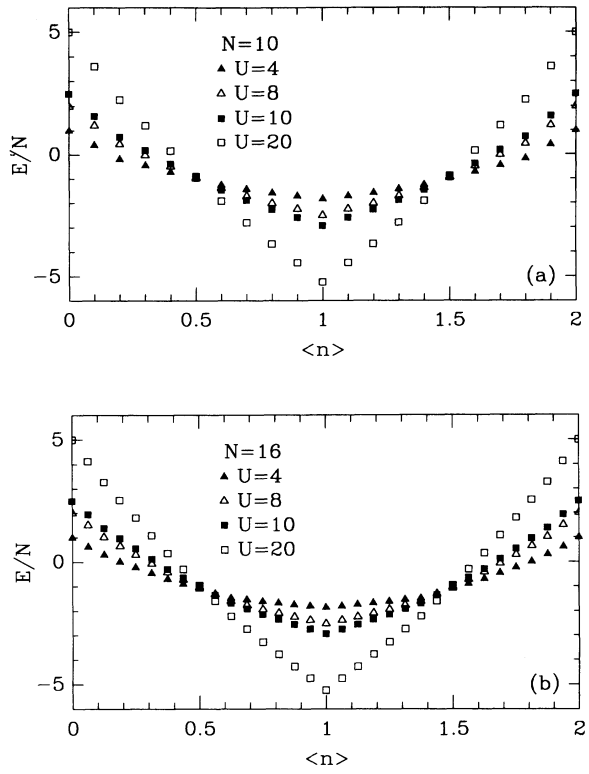

FIG. 6. (a) Energy (per site) of the ground state of the Hubbard model on a $\sqrt{10}\times\sqrt{10}$ cluster. (b) Same as (a) but for a 4×4 cluster.

TABLE I. Ground-state energy of the t-J model on a 4×4 cluster at different values of J ($t=1$). The energy of one electron is -4.

J	0 holes	1 holes	2 holes	3 holes	4 holes
2.0	−38.456 97	−34.929 66	−33.180 23	−30.510 55	−29.076 65
1.0	−19.228 48	−18.573 68	−18.806 14	−18.531 89	−18.852 63
0.8	−15.382 79	−15.352 83	−16.029 17	−16.273 46	−16.952 96
0.6	−11.537 09	−12.161 25	−13.312 17	−14.087 25	−15.117 65
0.4	−7.691 39	−9.013 63	−10.683 92	−11.996 85	−13.365 73
0.2	−3.845 70	−5.944 10	−8.211 81	−10.088 39	−11.911 98
0.1	−1.922 85	−4.467 86	−7.134 78	−9.315 65	−11.252 32

J	5 holes	6 holes	7 holes	8 holes	9 holes
2.0	−26.779 31	−26.062 65	−23.478 14	−21.638 68	−19.141 85
1.0	−18.763 71	−19.372 38	−18.315 37	−17.557 02	−16.196 86
0.8	−17.290 27	−18.131 82	−17.385 01	−16.834 68	−15.676 22
0.6	−15.874 22	−16.935 76	−16.498 98	−16.149 62	−15.179 79
0.4	−14.530 95	−15.796 05	−15.663 23	−15.504 96	−14.782 38
0.2	−13.287 18	−14.729 52	−14.883 01	−14.903 58	−14.411 48
0.1	−12.714 55	−14.229 83	−14.514 74	−14.619 80	−14.233 49

J	10 holes	11 holes	12 holes	13 holes	14 holes
2.0	−17.406 64	−14.700 14	−12.685 85	−10.000 00	−8.000 00
1.0	−15.133 16	−13.245 58	−11.639 60	−9.554 99	−7.760 89
0.8	−14.731 16	−12.989 37	−11.457 31	−9.476 52	−7.719 15
0.6	−14.387 64	−12.772 24	−11.283 77	−9.401 33	−7.679 22
0.4	−14.185 43	−12.622 69	−11.118 83	−9.329 32	−7.641 04
0.2	−13.990 39	−12.479 54	−10.962 31	−9.260 38	−7.604 51
0.1	−13.895 57	−12.410 35	−10.887 14	−9.227 03	−7.586 84

are presented on Table II for the 4×4 cluster. As can be observed from Fig. 6 there is no qualitative distinction between the weak- and strong-coupling regions regarding the curvature of the plots. This is a clear difference with respect to the *t-J* model where the actual value of J/t is important for phase separation. For the Hubbard model the curvature is mostly positive, being slightly negative only very close to half filling and between neighboring fillings, which indicates possible pairing[26] (with a small binding energy) but no phase separation. Results for the two lattice sizes are very similar and thus the finite-size effects for the ground-state energy seem small.

In Fig. 7 we present $\langle n \rangle$ vs μ at, e.g., $U/t=4$. Results for other values of U/t are qualitatively similar. In the case of the calculation performed using exact diagonalization techniques, the values of μ that make a given density stable are found as for the case of the *t-J* model. As observed in the figure, the states with odd number of particles cannot be made stable by tuning the chemical potential. The states with even number of electrons are all stable, showing that there is no phase separation in the model and that instead we having binding of holes. In the same figure we also show QMC results on a 4×4 lattice obtained directly in the grand-canonical ensemble where μ is the input parameter and $\langle n \rangle$ is measured as an output (and thus carries error bars). The Monte Carlo results have been obtained at finite but small temperatures. The agreement between the two techniques is good. For small densities we have also performed QMC calculations on larger clusters (up to 8×8 sites), showing that finite-size effects are small (although the "steps" observed at zero temperature are smeared out at finite temperature).[27]

Then, we conclude that, within the limitations of our calculations, there are *no* numerical indications of phase separation in the Hubbard model. An additional evidence in favor of this conclusion is provided by the analysis of the one-dimensional case. For the 1D *t-J* model, it is well known that at large J/t the system phase separates.[28] On the other hand, for the Hubbard model in 1D it has been shown in the bulk limit that there are

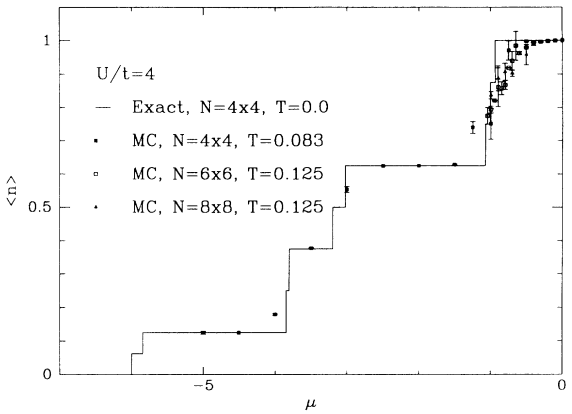

FIG. 7. Density $\langle n \rangle$ vs μ for the Hubbard model at $U/t=4$ using different techniques and clusters (T denotes temperature).

no discontinuities in the density of particles as a function of μ even at strong coupling and thus the system does *not* phase separate.[29] We believe that the same happens in two dimensions. Then, since the Hubbard and *t-J* models should describe the same physics at large U/t, our conclusion is that the *t-J* model does *not* phase separate at small J/t contrary to the results of Ref. 23. In the present analysis we find that phase separation for the 2D *t-J* model starts at $J/t \sim 1$, in good agreement with results obtained from a high-temperature expansion.[30]

VI. ELECTRONIC DENSITY OF STATES

The analysis of the electronic density of states in the new high-T_c superconductors as a function of doping is controversial. Photoemission spectroscopy (PES) and inverse photoemission spectroscopy (IPES) suggest that as the insulating state is doped, the gap region appears to be gradually filled in, with spectral weight transferred from both the lower valence band and the upper conduction bands of the undoped insulator.[31,32] The chemical potential μ of the doped metal was found to lie in the insulating gap, with μ roughly the same, relative to the valence

TABLE II. Ground-state energy of the Hubbard model on a 4×4 lattice at different values of U ($t=1$). The energy of one electron is −4.

Ne	$U=20$	$U=10$	$U=8$	$U=4$
16	−3.739 91	−7.029 00	−8.468 88	−13.621 85
15	−6.068 01	−8.893 01	−10.147 24	−14.665 24
14	−8.461 48	−10.807 01	−11.868 84	−15.744 59
13	−10.478 59	−12.463 13	−13.381 26	−16.727 00
12	−12.453 30	−14.164 38	−14.925 31	−17.729 58
11	−13.920 19	−15.513 72	−16.204 37	−18.648 33
10	−15.451 50	−16.903 56	−17.510 37	−19.580 94
9	−15.468 14	−16.551 23	−17.001 90	−18.553 63
8	−15.357 16	−16.143 21	−16.460 63	−17.534 90
7	−14.788 07	−15.345 37	−15.569 10	−16.320 54
6	−14.265 47	−14.595 84	−14.723 54	−15.136 01
5	−12.688 34	−12.932 26	−13.026 48	−13.332 83
4	−11.082 01	−11.256 21	−11.321 50	−11.530 29
3	−9.375 17	−9.493 70	−9.538 29	−9.681 24
2	−7.674 97	−7.740 18	−7.764 09	−7.838 93

and conduction band peaks, for *both* the electron and hole-doped materials. In other words, as the antiferromagnetic insulating state is doped, μ does *not* move across the gap if the doping is changed from holes to electrons.[31,33] On the other hand, oxygen x-ray absorption spectra measured on $La_{2-x}Sr_xCuO_4$ have been interpreted in terms of a picture in which hole doping introduces carriers into the lower band.[34] The observed two-peak absorption structure is identified as an upper peak arising from transitions into the upper band, while the lower peak is associated with holes doped into the top edge of the lower band. Similar experiments have been carried out[35] for electron-doped $Nd_{2-x}Ce_xCuO_4$ where only the upper band is observed. Then, x-ray absorption suggests that the chemical potential moves across the gap when the doping is changed from holes to electrons, in disagreement with PES experiments.[31] As was shown in the previous section, at zero temperature, we observe that a *finite* negative or positive shift of μ (approximately half the gap) is required to add holes or electrons to a half-filled Hubbard model. Once these values are exceeded, $\langle n \rangle$ appears to vary continuously with μ as the cluster size is increased. Then, from the analysis of the previous section, the Hubbard model gives results in agreement with x-ray experiments[34,35] rather than with PES experiments.[31]

Using Lanczos techniques, we have calculated the electronic density of states at finite doping on a $\sqrt{10}\times\sqrt{10}$ cluster for positive values of U in the Hubbard model.[36] Results for the t-J model are also presented on a 4×4 cluster while results for the attractive Hubbard model were discussed elsewhere.[36] More specifically, we have calculated

$$N_s^{(+)}(\omega)=\frac{1}{N}\sum_{\mathbf{k},n}|\langle\psi_n^{M+1}|c_{\mathbf{k}s}^{\dagger}|\psi_0^M\rangle|^2\delta(\omega-(E_n^{M+1}-E_0^M)), \tag{9}$$

and

$$N_s^{(-)}(\omega)=\frac{1}{N}\sum_{\mathbf{k},n}|\langle\psi_n^{M-1}|c_{\mathbf{k}s}|\psi_0^M\rangle|^2\delta(\omega+(E_n^{M-1}-E_0^M)) . \tag{10}$$

$N_s^{(+)}(\omega)$ is the density of states for adding an electron with spin s and energy ω and $N_s^{(-)}(\omega)$ is the density of states for removing an electron with spin s from a ground state with M electrons. N denotes the number of lattice sites, and the operator $c_{\mathbf{k}s}^{\dagger}=(1/\sqrt{N})\sum_j e^{i\mathbf{k}\cdot\mathbf{j}}c_{\mathbf{j}s}^{\dagger}$ creates a state with momentum $\mathbf{k}$ and spin s. $|\psi_0^M\rangle$ is the ground state of the subspace with M electrons and E_0^M is its energy. $|\{\psi_n^{M\pm1}\rangle\}$ denote states in the subspace with $M\pm1$ electrons and energies $\{E_n^{M\pm1}\}$. Figure 8 shows $N_{\uparrow}^{(+)}(\omega)$ (solid) and $N_{\uparrow}^{(-)}(\omega)$ (dashed) vs ω for $U/t=10$ (results for $U/t=20$ and 8 have been presented elsewhere[36]). The chemical potential μ (obtained from the previous section) is shown as a vertical line and moves from zero at half filling (ten electrons), Fig. 8(a), to the top edge of the lower Hubbard band, Fig. 8(a), when two electrons are removed (results for $s=\downarrow$ are identical to Fig. 8 for an even number of electrons in the ground state). Comparing Figs. 8(a) and 8(b), we observe that the effects of hole doping are to remove spectral weight from both the

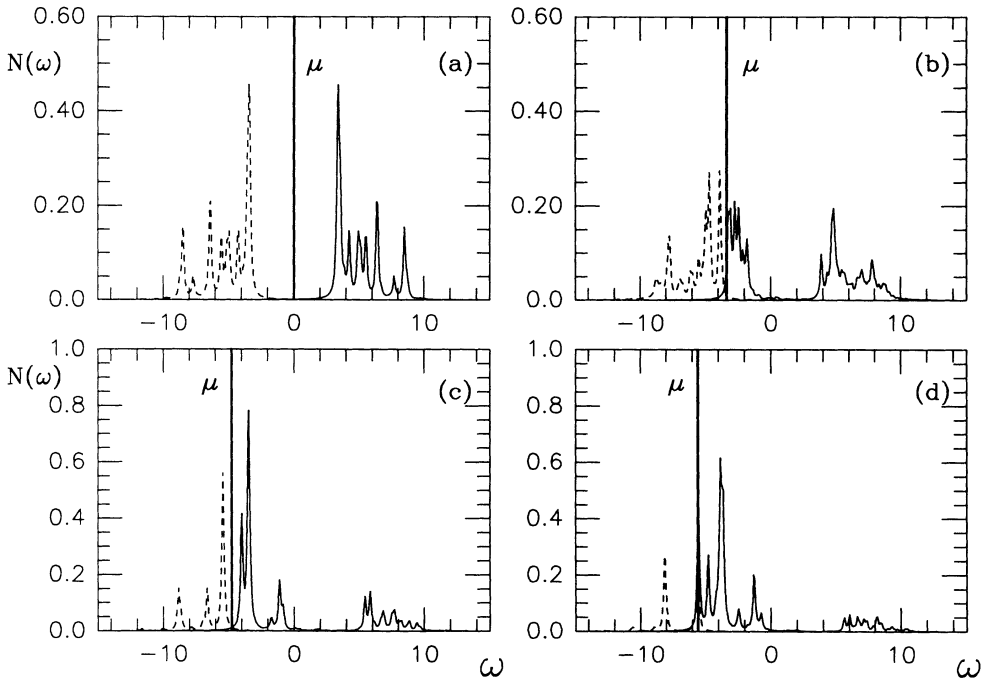

FIG. 8. Electronic spectral density of the Hubbard model $[N(\omega)=N_{\uparrow}^{(\pm)}(\omega)]$ on a $\sqrt{10}\times\sqrt{10}$ cluster at $U/t=10$. The solid lines correspond to $N_{\uparrow}^{(+)}(\omega)$ while the dashed lines denote $N_{\uparrow}^{(-)}(\omega)$. (a) Results at half filling, corresponding to $x=0$; (b) at $x=0.2$; (c) at $x=0.4$; and (d) at $x=0.6$. The solid thick vertical line indicates the position of μ. The δ functions have a finite width produced by a small shift of the poles from the real axis.

upper and lower Hubbard bands and to create additional density of states in the gap, starting at the edge of the lower Hubbard band. Results for further dopings are shown in Figs. 8(c) and 8(d). With this additional doping, the chemical potential moves slowly down from its value with eight electrons, and further spectral weight is removed from both the upper and lower Hubbard bands, towards the gap region above the lower Hubbard band.[37] When U is of the order of the bandwidth $8t$, we found that the spectral weight created in the gap region by doping fills the gap (although with small spectral weight).[36] A connection between these results and those found for the optical conductivity will be made in the next section. For smaller values of U/t (Fig. 9) the gap disappears and there is no distinction between the upper band and the new band immediately after the chemical potential. Due to particle-hole symmetry, the results for adding electrons to the half-filled cluster are given by simply reflecting Figs. 8 and 9 about the $\omega=0$ axis.

How is the spectral weight distributed in Fig. 8? The spectral weight of $N_{\uparrow}^{(-)}(\omega)$ is *exactly* $(1-x)/2$ since $\int_{-\infty}^{\infty} d\omega\, N_{\uparrow}^{(-)}(\omega)$ is equal to the number of particles in the state $|\psi_0^M\rangle$ with spin $\uparrow$ per site. The spectral weight in the IPES region of the spectrum is identically equal to $(1+x)/2$ since the sum rule states that $\int_{-\infty}^{+\infty} d\omega[N_{\uparrow}^{(-)}(\omega)+N_{\uparrow}^{(+)}(\omega)]=1$. We observed numerically that for large U/t, the spectral weight per spin of the new states ($I_{\rm new}$) created in the gap immediately after the chemical potential increases approximately linearly with x. The slope of the curve $I_{\rm new}$ vs x converges to one as U/t is increased in agreement with predictions in the strong-coupling limit.[38] For finite U/t the slope is *larger* than one (at small x) and increases when U/t is reduced, at least for U/t large where a genuine gap exists in the IPES spectrum.

Thus we find, as seen in PES experiments,[31] that doping a half-filled Hubbard cluster does not simply produce a rigid shift of the density of states relative to the Fermi level, but rather, new states are created in the gap. However, in contrast to the same PES experiments[31] and in agreement with x-ray absorption experiments,[34,35] the chemical potential for the Hubbard model moves across the gap when the doping is changed from holes to electrons, lying near the top of the lower Hubbard band when holes are added and near the lower part of the upper Hubbard when electrons are added. A similar $\langle n \rangle$ vs μ behavior as observed in Fig. 7 exists when the gap is a charge-transfer gap.[39] Then, we believe that the jump of μ from the top of the lower band to the bottom of the upper band as holes or electrons are added to a half-filled band is a general property of strongly correlated electronic models with repulsive Coulomb interactions.[40] This disagreement with PES experiments[31] could mean that the n-type materials are actually producing *hole* doping on the Cu-O planes or that Hubbard-like models are missing some essential feature needed to describe properly the physics of the superconductors.

For completeness, we have performed a similar calculation for the t-J model on a 4×4 cluster.[41] In Figs. 10(a)–10(c) we show results at $J/t=0.4$ and various doping fractions. In the t-J model double occupancy is not allowed and thus there is no upper Hubbard band in our results. The qualitative behavior of the chemical potential is similar to that found in the Hubbard model. With respect to the distribution of spectral weight, for the t-J model the sum rule is modified to $\int_{-\infty}^{+\infty} d\omega[N_{\uparrow}^{(-)}(\omega)+N_{\uparrow}^{(+)}(\omega)]=(1+x)/2$, due to the constraint of no double occupancy. Since $\int_{-\infty}^{\infty} d\omega N_{\uparrow}^{(-)}(\omega)=(1-x)/2$ (i.e., the number of particles in the ground state with a given spin), then the IPES

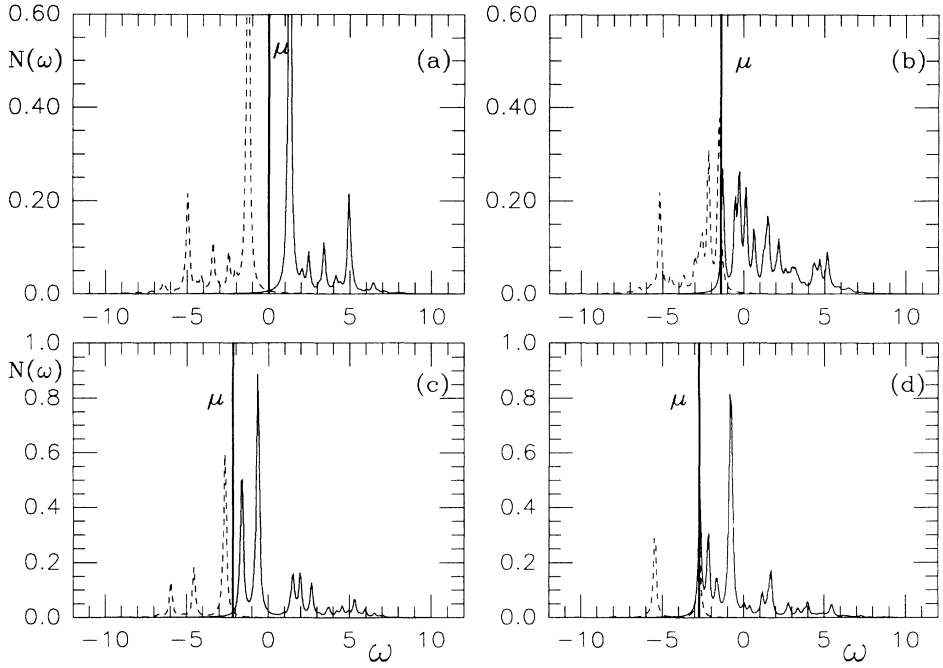

FIG. 9. Same as Fig. 8 but for $U/t=4$.

spectral weight right above μ is *exactly* equal to x, in agreement, with the strong-coupling results of Sawatzky.[38] As remarked above, the double occupancy in the Hubbard model introduces more spectral weight in the region immediately after the chemical potential than what is allowed in the t-J model.

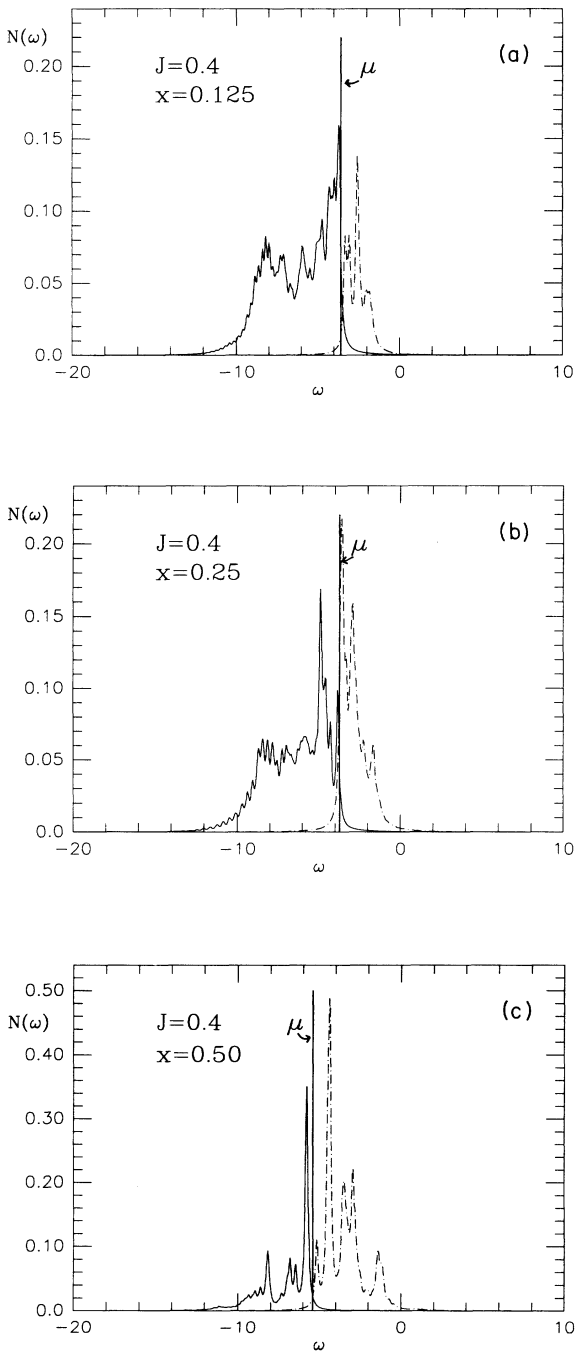

FIG. 10. (a) Electronic spectral density of the t-J model $[N(\omega)=N_{\uparrow}^{(\pm)}(\omega)]$ on a 4×4 cluster at $J=0.4$ ($t=1$). The dot-dashed lines correspond to $N_{\uparrow}^{(+)}(\omega)$ while the solid lines denote $N_{\uparrow}^{(-)}(\omega)$. The hole doping is $x=1-M/N=0.125$. The solid thick vertical line indicates the position of μ. (b) Same as (a) but for $x=0.25$. (c) Same as (a) but for $x=0.50$.

VII. OPTICAL CONDUCTIVITY

The real part of the optical conductivity, $\sigma_1(\omega)$, provides useful information about the electronic structure of the cuprate superconductors.[42–44] The reflectivity is measured over a wide frequency range and the results are Kramers-Kronig transformed to obtain the optical conductivity as a function of ω. Typical results show that in the insulating phase ($x=0$), $\sigma_1(\omega)$ has negligible absorption below the CT gap of ~ 1.5–2.0 eV. When the CuO_2 plane is doped with holes or electrons, there is a rapid growth of spectral weight at low frequencies creating a $\omega=0$ Drude-like peak due to mobile carriers (that grows like x) and a broad mid-infrared (ir) feature in the region $0.1\ \text{eV}<\omega<0.5$ eV (approximately doping independent), while the spectral weight in the CT band decreases.[43,44] The reported integrated conductivity in $La_{2-x}Sr_xCuO_4$ up to 4 eV remains approximately constant with doping showing that spectral weight is redistributed from the charge-transfer band to lower frequencies. A measure of this transfer of spectral weight used in several experimental papers,[43,44] is a normalized effective carrier density N_{eff} proportional to the integral of $\sigma_1(\omega)$ up to the gap (~ 1.5 eV). This quantity was found to rise more rapidly than would be expected from the doped carrier concentration alone. This qualitative behavior was found in both p-type[44] ($La_{2-x}Sr_xCuO_4$) and n-type[43] ($Pr_{2-x}Ce_xCuO_4$) superconductors. These experimental features of the optical conductivity have been described as "anomalous."

Can these results be understood within the framework of the theoretical models presently used to describe the Cu-O superconductors? In this section we study this question for the one-band Hubbard model where, as stated before, it is assumed that the lower (upper) Hubbard band corresponds to the O $2p$ (Cu $3d$) band of the cuprates and thus the CT gap can be described by an "effective" Hubbard coupling U/t. Monte Carlo calculations of the momentum occupation[45] $\langle n_k \rangle$ in the doped region are consistent with a large Fermi surface enclosing $1-x$ electrons. A natural question is whether such a model can exhibit the observed doping dependence of $\sigma_1(\omega)$. Using Lanczos techniques, we calculate $\sigma_1(\omega)$ and the Drude weight for finite clusters.[46] We find that the behavior of the doped Hubbard model is similar to the experimental results clearly exhibiting a transfer of spectral weight from above the gap to the Drude peak and the mid-ir region.[47]

$\sigma_1(\omega)$ can be decomposed into a zero-frequency Drude weight δ function and a regular part,

$$\sigma_1(\omega)=D\delta(\omega)+\frac{\pi e^2}{N}\sum_{n\neq 0}\frac{|\langle n|j_x|0\rangle|^2}{E_n-E_0}\delta(\omega-(E_n-E_0))\ . \tag{11}$$

where j_x is the paramagnetic current operator

$$j_x=it\sum_{i,s}(c^{\dagger}_{i+xs}c_{is}-c^{\dagger}_{is}c_{i+xs})\ ,$$

e is the electric charge, and N is the number of sites of the lattice. $\{|n\rangle\}$ denote states of energy $\{E_n\}$, which are

excited when the current operator acts on the ground state $|0\rangle$ (whose energy is E_0). Using the f-sum rule for the Hubbard model,[48]

$$2\int_0^\infty \sigma_1(\omega)d\omega=\frac{\pi e^2}{2N}\langle 0|(-T)|0\rangle \ , \tag{12}$$

where the kinetic energy operator T is the first term in Eq. (1), one obtains[49,50]

$$\frac{D}{2\pi e^2}=\frac{1}{4N}\langle 0|(-T)|0\rangle-\frac{1}{N}\sum_{n\ (\neq 0)}\frac{|\langle n|j_x|0\rangle|^2}{E_n-E_0} \ . \tag{13}$$

Using Lanczos techniques on $\sqrt{10}\times\sqrt{10}$ and 4×4 periodic clusters, we have independently calculated the regular part of $\sigma_1(\omega)$ [whose integral corresponds to the second term on the right-hand side of Eq. (13)] and the kinetic energy, obtaining D from Eq. (13).

Results showing $\sigma_1(\omega)$ vs ω for $U/t=10$ on a 4×4 cluster as various dopings are shown in Fig. 11. The results for the $\sqrt{10}\times\sqrt{10}$ cluster are qualitatively similar. At half filling, the insulating Hubbard gap is clearly visible. There is no spectral weight in the interval $0\le\omega\le6.3t$. Upon doping, spectral weight is transferred from the region above the Hubbard gap to the Drude peak at $\omega=0$ and to the midgap region. For doping $x=0.125$, 36% of the total weight is below the gap while for higher dopings of $x=0.25$ and 0.375, the percentages are 87% and 94%, respectively.

The presence of the mid-infrared band is clear in our results and thus its existence can be accounted for within the context of a simple one-band Hubbard model in two dimensions as previously remarked.[46] Note that similar calculations in 1D have not observed such a large spectral weight in the mid-gap region[51,52] and thus its presence is a two- (or higher-) dimensional effect. At $x=0.125$ the insulating gap is almost filled since the mid-ir region has a total width comparable with the gap itself.[53] Actually, this is similar to the results for the single-particle spectral weight, $N(\omega)$, in Sec. VI, that showed that hole doping removed single-particle spectral weight from both the upper and lower Hubbard bands and created additional states in the gap extending upwards from the lower Hubbard band. We believe that the new states found in $N(\omega)$ and those found in the mid-gap region of $\sigma_1(\omega)$ have a similar origin, i.e., the distortions created by holes in an antiferromagnetic background, "string states," which only exist in two or higher dimensions.[8,20] Variational states having the correct short-distance correlations should be able to reproduce these results.

For small values of the coupling $U/t\sim4$, we found that the upper Hubbard band and the mid-ir band can hardly be distinguished upon doping. Thus, in order to reproduce experiments [where the upper and midgap bands appear as separate features of $\sigma_1(\omega)$], it is necessary to work roughly in the region $U/t>4$. Another constraint on U/t is set by the observation that the total spectral weight below 4 eV is approximately independent of doping.[43] The kinetic energy of the Hubbard model which determines this spectral weight through the f-sum rule is shown in Fig. 12(a) for various values of U/t. For large values of U/t, there is a significant change in the total spectral weight with doping which is not compatible with experiments. For example, at $U/t=20$ the kinetic

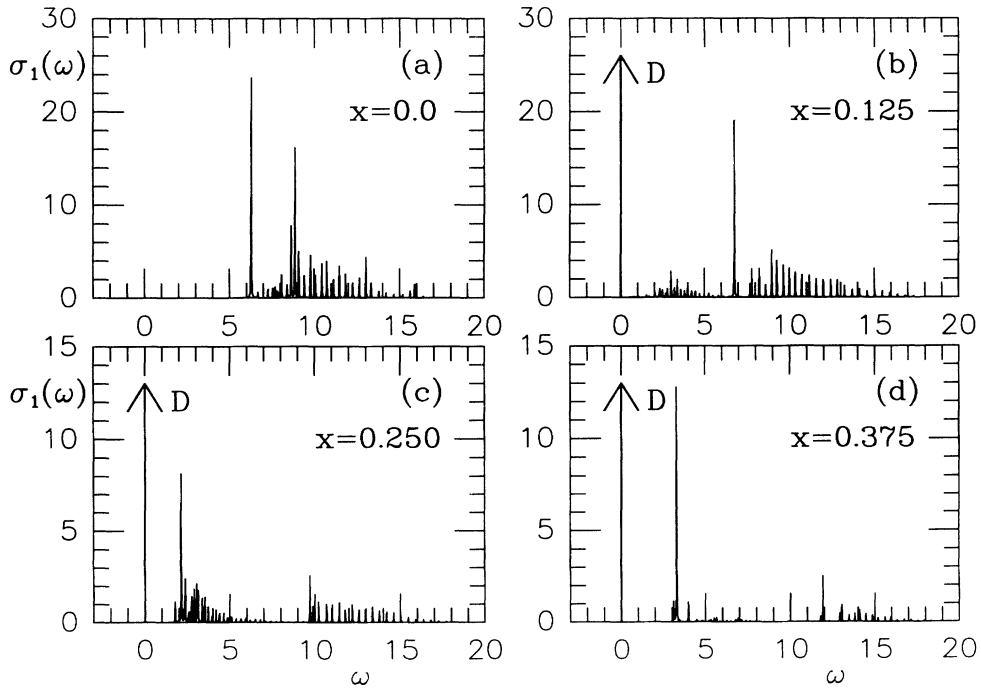

FIG. 11. The real part of the optical conductivity $\sigma_1(\omega)$ for a 4×4 cluster with $U/t=10$ and band fillings (a) $x=0$ (half-filled band), (b) $x=0.125$, (c) $x=0.250$, and (d) $x=0.375$. A small shift from the real axis ($\epsilon=0.01$) was used to plot the δ functions. The peak at $\omega=0$ represents the Drude peak (D). Its intensity in the figure is *not* proportional to its real magnitude, but it is included only for illustration.

energy changes by more than a factor of 2 with respect to half filling, when the system is doped to $\langle n \rangle = 0.6$. This change is even larger if U/t is further increased. Thus, to satisfy both the structure in $\sigma_1(\omega)$ and the behavior of the spectral weight one is led to an intermediate coupling U of order the bandwidth.[54]

Figure 12(b) shows the Drude weight $D_n = D/2\pi e^2$ vs $\langle n \rangle$ for various values of U/t and $\sqrt{10}\times\sqrt{10}$ and 4×4 site clusters. As discussed by Kohn,[49] one expects that in an insulating phase D will vanish as $\exp(-N_x/\xi)$ as the linear size N_x of the system increases, as recently seen for 1D Hubbard rings.[51] This is in agreement with our results at half filling where $|D|$ is a small number.[55] Figure 12(b) shows that as the system is doped towards quarter filling $\langle n \rangle = 0.5$, the Drude weight grows rapidly. Increasing the doping further, the system becomes a gas of noninteracting electrons and the Drude weight follows the kinetic energy. For very large couplings (but not as large as to induce a transition to a ferromagnetic phase), the Drude weight approximately converges to the result shown in Fig. 12(b) for $U/t = 100$. Note that the curve D_n vs doping is smooth and the results for $\sqrt{10}\times\sqrt{10}$ and 4×4 sites are close to each other and thus we believe its qualitative shape will survive in the bulk limit. Note also that Fig. 12(b) tells us whether the conduction is made by holes or electrons. Near half filling, D grows proportional to x, which is compatible with a picture of weakly interacting holes being the carriers. On the other hand, for large doping of holes, D is proportional to $1-x$, this time compatible with a gas of noninteracting electrons. Then, we believe that the change in the sign of the slope of D vs x at approximately quarter filling may be taken as an indication that the nature of the carriers changes. Although this is not a rigorous statement, we believe that the Hall coefficient will change sign also in the neighborhood of quarter filling.

In Fig. 13 we show the sum of the Drude spectral D and the midgap spectral weight under $\sigma_1(\omega)$. Normalizing this weight by dividing it by $\pi e^2 t$ gives an effective carrier density in which the unrenormalized mass is $m = (2t)^{-1}$, i.e.,

$$N_{\text{eff}} = \frac{1}{\pi e^2 t} \int_0^{\omega_c} \sigma(\omega) d\omega \ . \tag{14}$$

Here ω_c is a frequency just below the upper Hubbard band. The dependence of N_{eff} vs x is shown in Fig. 13 for several values of U/t. For smaller values of U/t, more spectral weight is transferred upon doping. An important feature, clearly seen in Fig. 13, is that as the system is doped away from half filling, it is the number of holes x that determines the spectral weight and not the total number of electrons as would be the case for the noninteracting system. The dependence of N_{eff} vs x is qualitatively similar to that observed experimentally,[43,44] although the experimental results rise more rapidly with x. Since the data presented here are a first-principles calculation with only *one* free parameter U/t of a very simplified model, we consider Fig. 13 as an encouraging step forward in comparing experiments with Hubbard model predictions.

For completeness, we have studied the optical conductivity of the t-J model at all doping fractions.[56] The sum

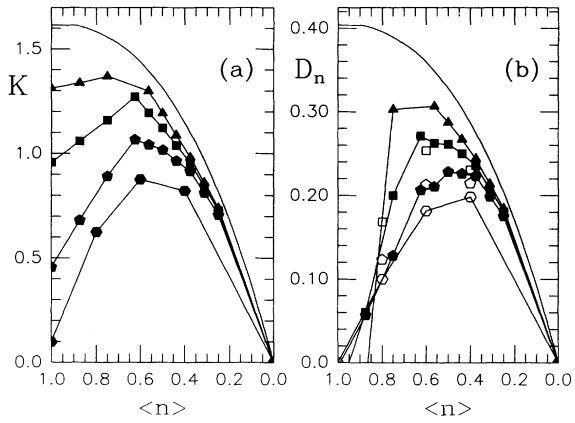

FIG. 12. (a) Kinetic energy per site of the Hubbard model $K = \langle 0|(-T)|0\rangle/N$ on a 4×4 cluster as a function of doping for $U/t = 4$ (full triangles), $U/t = 8$ (full squares), and $U/t = 20$ (full pentagons). We also show results for a $\sqrt{10}\times\sqrt{10}$ sites cluster at $U/t = 100$ (full hexagons). The solid line without points corresponds to results for $U/t = 0$ in the bulk limit. (b) $D_n = D/(2\pi e^2)$ vs x for various couplings U/t. Full triangles, squares, and pentagons denote results for $U/t = 4$, 8, and 20, respectively, on a 4×4 lattice. Open squares, pentagons, and hexagons indicate results for a $\sqrt{10}\times\sqrt{10}$ site cluster at $U/t = 8$, 20, and 100 respectively. The solid line without points denotes the results for $U/t = 0$ in the bulk limit. The fact that D is negative near half filling is a known finite-size effect previously discussed in the literature (see Refs. 51 and 55).

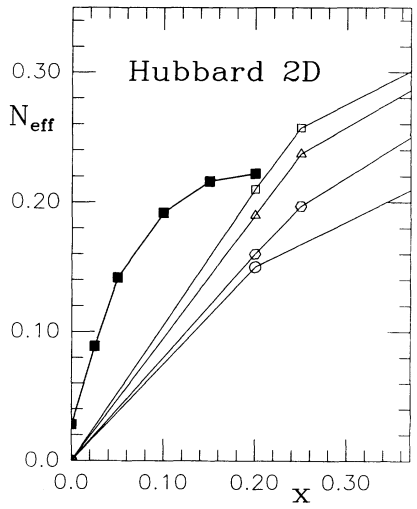

FIG. 13. N_{eff} (i.e., the sum of the Drude weight and the midband weight) vs doping for various values of U/t. Open squares corresponds to $U/t = 8$, open triangles to $U/t = 10$, open hexagons to $U/t = 20$, and the circles to $U/t = 200$. Doping of $x = 0.25$ ($x = 0.20$) corresponds to a 4×4 ($\sqrt{10}\times\sqrt{10}$) sites cluster. The full squares correspond to the experimental results for $La_{2-x}Sr_xCuO_4$ taken from Ref. 43. Not shown in the figure are results for larger dopings that produce the "kinks" in the curves at $x = 0.25$.

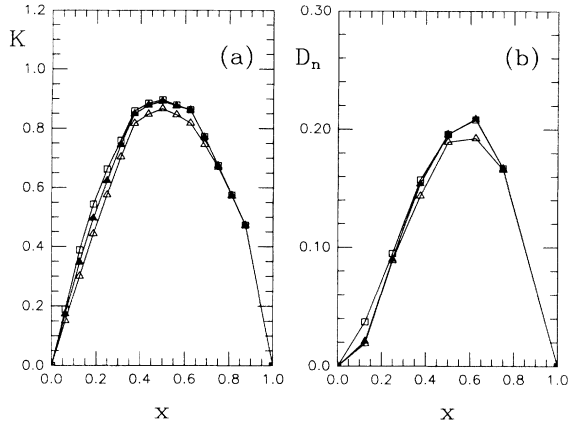

FIG. 14. (a) Kinetic energy per site of the t-J model $K=\langle 0|(-T)|0\rangle/N$ on a 4×4 cluster as a function of doping for $J/t=0.1$ (□), $J/t=0.4$ (▲), and $J/t=1.0$ (△). (b) $D_n=D/(2\pi e^2)$ vs x for various couplings J/t. △, ▲, and □ denote $J/t=1.0$, 0.4, and 0.1 respectively, on a 4×4 lattice.

rule Eq. (12) is valid also for this model. In Fig. 14(a) we show the kinetic energy per site on a 4×4 cluster as a function of doping for different values of J/t. In Fig. 14(b) we show the Drude weight $D/2\pi e^2$ also a function of doping for various couplings. The general trend of these results is similar to those of the Hubbard model at large U/t although the presence of three-site terms in the t-J may be important to account for the U/t dependence of the Drude weight.[57] D increases with doping, at small x. For example, with two holes ($x=0.125$) the spectral weight at $\omega=0$ is 38.4% and 24.2% for $J/t=0.1$ and 0.4, respectively.[58] Note that since at half filling there are no carriers, the kinetic energy vanishes at $x=0$. In general the Drude weight and $\langle T\rangle$ have a very similar behavior. The results are almost independent of the coupling J/t.

Summarizing this section, we have calculated the optical conductivity of the two-dimensional Hubbard and t-J models on clusters of $\sqrt{10}\times\sqrt{10}$ and 4×4 sites. For $U>0$, we found in the undoped case a gap in the spectrum. Upon doping, spectral weight is shifted to the Drude peak and the mid-infrared region. The intensity of the Drude peak grows quickly with doping. These features are in good qualitative agreement with experiments if a coupling constant U/t of the order of the bandwidth is selected. Then, our results provide additional evidence that the intermediate region of parameters U/t is the most relevant for describing these superconductors.[59]

VIII. SEARCHING FOR SUPERCONDUCTIVITY

The most important feature of these new high-T_c materials that we expect to understand theoretically is their superconducting phase. There are many ways to search for indications of superconductivity in the t-J or Hubbard models. In this section we will consider the equal-time pairing correlation function $\chi_{\rm sup}$ defined as

$$\chi_{\rm sup}=\frac{1}{N}\sum_{\rm i,j}\langle\Delta(\mathbf{i})\Delta^{\dagger}(\mathbf{j})\rangle\ , \tag{15}$$

where $\langle\cdots\rangle$ denotes the expectation value in the ground state corresponding to a given coupling and doping fraction x. The pairing operator for the t-J model is $\Delta(\mathbf{i})=\sum_{\hat\delta}\bar c_{\mathbf{i},\uparrow}\bar c_{\mathbf{i}+\hat\delta,\downarrow}f(\hat\delta)$ and $\hat\delta=\pm\mathbf{x},\pm\mathbf{y}$ ($\mathbf{x}$ and $\mathbf{y}$ being unit vectors in the crystal directions). $f(\hat\delta)$ (which defines the rotational symmetry of the operator) takes the values[60] $f(\pm\mathbf{y})=1,-1$ [$f(\pm\mathbf{x})=1$] for extended s waves and d waves, respectively, while for p_x waves $f(\pm\mathbf{y})=0$, $f(\pm\mathbf{x})=\pm1$.

It is important to subtract from $\chi_{\rm sup}$ the contribution of disconnected diagrams[61] given by

$$\bar\chi_{\rm sup}=\frac{1}{N}\sum_{\mathbf{i},\mathbf{j},\hat\delta,\hat\delta'}\langle\bar c_{\mathbf{i},\uparrow}\bar c^{\dagger}_{\mathbf{j},\uparrow}\rangle\langle\bar c_{\mathbf{i}+\hat\delta',\downarrow}\bar c^{\dagger}_{\mathbf{j}+\hat\delta,\downarrow}\rangle f(\hat\delta)f(\hat\delta')\ . \tag{16}$$

The difference between $\chi_{\rm sup}$ and $\bar\chi_{\rm sup}$ is defined as the "connected" part ($\chi^c_{\rm sup}$) of the correlation function and it is the quantity of physical interest. If $\chi^c_{\rm sup}>0$, then pairing correlations are said to be "enhanced," although this is not enough to show the existence of a superconducting phase in the model. If such a phase exists then $\chi^c_{\rm sup}$ should grow like the volume of the lattice in a finite-size scaling analysis. In Fig. 15 we show $\chi^c_{\rm sup}$ at $J/t=0.3$ for s and d waves as a function of doping x. Results at other couplings between $J/t=2.0$ and 0.1 are qualitatively similar. $\chi^c_{\rm sup}$ corresponding to p-wave order is suppressed at all values of J/t and doping. The most important features of Fig. 15 is the enhancement of $\chi^c_{\rm sup}$ at small and intermediate doping fractions. At low doping, both s and d waves are enhanced,[62] while for dopings roughly between 20% and 40% only the s wave is attractive. The enhancement of the d-wave correlation near half filling is in agreement with previous calculations.[63] Beyond $\sim$20% doping the existence of a different region where only the s-wave correlations are enhanced is in agreement with recent QMC results for the Hubbard model.[61,11] Since experimentally these high-T_c materials seem to have s-wave superconductivity, it is important to explore this type of pairing symmetry in simple models. Although the doping at which this s-wave region exists is

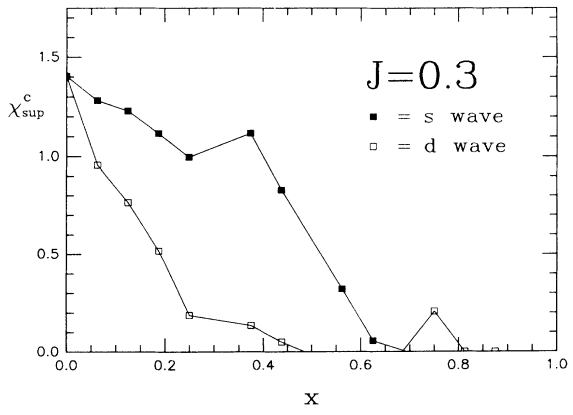

FIG. 15. Connected pairing correlation $\chi^c_{\rm sup}$ at $J=0.3$ and $t=1$ on a 4×4 lattice. Results are shown for s- and d-wave correlations.

large, we do not know if the t-J model is a *quantitative* model of high-T_c materials. Experimentally, it is only when the AF correlations are mostly suppressed that superconductivity appears.

Is Fig. 15 an indication of superconducting LRO? Although only studies on larger lattices can conclusively answer this question, we believe that Fig. 15 does *not* imply LRO superconductivity for the following reasons: (a) for 0 and 1 hole we have explicitly studied the function $C(\mathbf{i}-\mathbf{j})=\langle \Delta^{\dagger}(\mathbf{i})\Delta(\mathbf{j})\rangle$ vs $|\mathbf{i}-\mathbf{j}|$. We found that $C(\mathbf{i}-\mathbf{j})$ quickly decays with distance. Actually the contributions coming from *short* distances, i.e., $|\mathbf{i}-\mathbf{j}|=0$ and 1 account for 100% (97%) of $\chi^c_{\rm sup}$ in the zero hole (one hole) subspace. Note also that there is *no* enhancement of $\chi^c_{\rm sup}$ increasing doping at a fixed J/t, but rather the s- and d-wave correlations drop with x (the d wave faster than the s wave). Since at $x=0$ we know that the system does not superconduct and away from it, $\chi^c_{\rm sup}$ is not enhanced, then there are no obvious indications of LRO superconductivity due to doping; (b) we have compared our results with recent QMC simulations for the Hubbard model.[61] At $U/t=10$ (i.e., $J/t=0.4$) the agreement between the two techniques is *excellent* on a 4×4 lattice. With QMC it has been found[61] that the pairing correlations for a 4×4 lattice at $U/t=4$ and 10 are qualitatively similar and that results for 4×4 and 6×6 lattices are almost identical showing *no* increase in $\chi^c_{\rm sup}$ with the lattice size.

Then, we believe that the large pairing correlations we have found are a *short*-distance effect. Actually it can be easily shown that $C(\mathbf{i}-\mathbf{j})$ at short distances (especially the case $\mathbf{i}=\mathbf{j}$) can be rewritten in terms of spin-spin or spin-hole operators which are unrelated to superconductivity. These operators are related with spin order and they are enhanced when the temperature is reduced simply because short-distance spin correlations are enhanced. We believe that a similar problem occurred in earlier QMC calculations performed in the Hubbard model where claims of enhancement of d-wave pairing susceptibilities at low temperatures were reported. This enhancement came from short-distance spin-spin correlations rather than actual long-range pairing correlations. To further support these results, we shown in Fig. 16 the actual decay of the pairing-pairing correlation $C(\mathbf{r})$ as a function of distance for different lattice sizes using a QMC simulation.[64] From this plot it is clear that already at distances of two lattice spacings, the signal is zero within the statistical error bars and thus no indications of long-range order can be observed. We remark that analyzing the actual decay of the correlation function [rather than its zero momentum component, which is the sum $\sum_{\mathbf{r}}C(\mathbf{r})$] is very important and has not been properly emphasized before. Some operators may show enhancement at short distances as a function of different parameters producing a net enhancement in $\sum_{\mathbf{r}}C(\mathbf{r})$, while at large distances their behavior is unchanged or even suppressed. In the next section we discuss an example related with chiral order.

Thus, this numerical analysis for the 2D t-J and Hubbard models does *not* show clear indications of superconductivity. Different groups working with different models and techniques are reaching similar negative conclusions.[61,65] We would like to conclude this section commenting on possible ways to circumvent our results regarding superconductivity in the Hubbard and t-J models. One obvious criticism is that the lattices used in our study are too small to look for superconductivity. That certainly applies to the t-J model on a 4×4 lattice where few pairs can be accommodated. The argument is less solid for QMC simulations on the Hubbard model where 8×8 lattices have been analyzed, although they have been performed at finite temperature and it may occur that the critical temperature of these models is very low. However, recently it has been claimed that a Monte Carlo simulation performed at strictly zero temperature has produced also negative conclusions regarding superconductivity.[66] These results suggests that perhaps we have to introduce modifications in the Hubbard model to produce a truly superconducting phase at low temperature and finite doping. Nonetheless, it is puzzling to observe that while many of the *normal* state properties of these superconducting materials are at least qualitatively reproduced by Hubbard-like models (as shown in Secs. IV, VI, and VII), the superconducting phase is still missing.

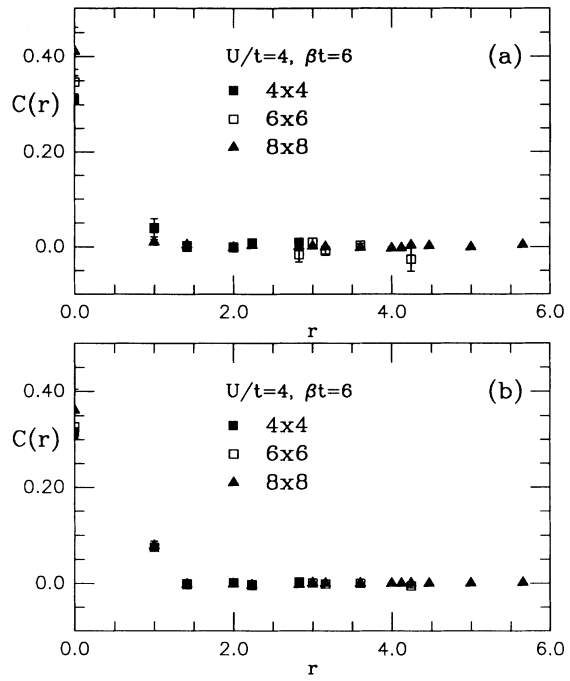

FIG. 16. Pairing-pairing correlation functions of the Hubbard model at $U/t=4$ and temperature $T=t/6$ on lattices of different sizes. (a) corresponds to d-wave symmetry, while (b) is s wave. The doping fraction $\langle n\rangle$ is 0.83, 0.90, and 0.84, for the 4×4, 6×6, and 8×8 clusters, respectively.

Recently, another possibility has been presented in order to explain the absence of positive numerical results for superconductivity in the Hubbard model. The idea[67] is that the pairing operators used in Monte Carlo simulations produce a very weak signal that may be hidden in the statistical noise. Suppose that the fermionic operators $c_{\mathbf{k},s}$ acting over the ground state of the system creates a state which has a very small overlap Z with states created by dressed "quasiparticle" operators $\gamma_{\mathbf{k},s}$.

In such a case, there will be an intrinsic suppression factor Z^2 in the Monte Carlo signal for pairing-pairing correlation functions when "bare" rather than dressed operators are used. It has been shown numerically that the overlap Z is indeed small.[67] Thus, additional quasiparticle operators should be constructed producing a larger Z factor and different pairing operators $\sum_{\mathbf{k},s} f(\mathbf{k})\gamma_{\mathbf{k},s}\gamma_{-\mathbf{k},-s}$ should be used in Monte Carlo studies [$f(\mathbf{k})$ being a properly selected function of momentum]. We strongly encourage a careful study of this possibility.

IX. SEARCHING FOR FLUX AND CHIRAL STATES IN THE *t-J* MODEL

Among the many candidate ground states for strongly correlated electronic models at finite doping, the existence of states that break time reversal and parity symmetries has been raised. Although there are no clear examples of realistic Hamiltonians having ground states with these properties, it is nevertheless interesting to search for indications of this exotic type of spin order in the *t-J* model.[68] For that purpose we have considered different order parameters starting with the *uniform* chiral state.[69] Define

$$\Gamma_{\mathbf{i}}(\hat{\delta},\hat{\delta}') = \mathbf{S}_{\mathbf{i}} \cdot (\mathbf{S}_{\mathbf{i}+\hat{\delta}} \times \mathbf{S}_{\mathbf{i}+\hat{\delta}+\hat{\delta}'}) , \tag{17}$$

and its associated zero-momentum correlation $\chi_{\rm ch} = \langle (1/N)(\sum_{\mathbf{i}} \Gamma_{\mathbf{i}})^2 \rangle$. If $\langle \Gamma \rangle \neq 0$ then parity (reflections) and time-reversal symmetries are spontaneously broken. Consider also the plaquette operators[70]

$$\begin{aligned} O_{\mathbf{i}} &= \mathrm{Im\,Tr}(\chi_{\mathbf{i},\mathbf{i}+\mathbf{x}}\chi_{\mathbf{i}+\mathbf{x},\mathbf{i}+\mathbf{x}+\mathbf{y}}\chi_{\mathbf{i}+\mathbf{x}+\mathbf{y},\mathbf{i}+\mathbf{y}}\chi_{\mathbf{i}+\mathbf{y},\mathbf{i}}) \\ &= \Gamma_{\mathbf{i}}(\mathbf{x},\mathbf{y}) n_{\mathbf{i}+\mathbf{y}} + \Gamma_{\mathbf{i}+\mathbf{x}}(\mathbf{y},-\mathbf{x}) n_{\mathbf{i}} \\ &\quad + \Gamma_{\mathbf{i}+\mathbf{y}}(-\mathbf{y},\mathbf{x}) n_{\mathbf{i}+\mathbf{x}+\mathbf{y}} + \Gamma_{\mathbf{i}+\mathbf{y}+\mathbf{x}}(-\mathbf{x},\mathbf{y}) n_{\mathbf{i}+\mathbf{x}} , \end{aligned} \tag{18}$$

where $\chi_{\mathbf{i},\mathbf{j}} = \sum_s c^{\dagger}_{\mathbf{i},s} c_{\mathbf{j},s}$; Tr means that we sum over the four equivalent plaquette operators obtained by a cyclic permutation of indices and its associated correlation is $\chi_{\rm pl} = \langle (1/N)(\sum_{\mathbf{i}} O_{\mathbf{i}})^2 \rangle$. A nonzero value of $\langle O \rangle$ would signal a symmetry breaking pattern similar to $\langle \Gamma \rangle$ with the advantage that it is explicitly rotational invariant (while Γ breaks $\pi/2$ rotations). In Figs. 17(a) and 17(b) we show $\chi_{\rm ch}$ and $\chi_{\rm pl}$ vs doping for different values of J/t. We know that at half filling (or with static holes) there is no chiral order since the ground state is Néel-like (thus the value of $\chi_{\rm ch}$ at $x=0$ is considered a "small' number). Then, if this type of order is actually enhanced with doping, we should expect an increase in $\chi_{\rm ch}$. However, Fig. 17(a) shows that chiral order is actually suppressed by doping. This tendency is even *stronger* reducing J/t as suggested by mean-field studies.[71] The uniform *plaquette* operator is more involved. Note that in Fig. 17(b) at $x \sim 0.12$, $\chi_{\rm pl}$ seems enhanced at $J/t = 0.3$. However, consider the correlation function $C_{\rm pl}(\mathbf{i},\mathbf{j}) = \langle \frac{1}{2}(O_{\mathbf{i}}O_{\mathbf{j}} + O_{\mathbf{j}}O_{\mathbf{i}}) \rangle$ vs $|\mathbf{i}-\mathbf{j}|$. We found that the increase of $\chi_{\rm pl}$ for two holes is a *short*-distance effect produced by an increase in a factor of ~ 2 and 3 of the zero-distance correlation $C_{\rm pl}(0,0) = \langle O_{\mathbf{i}}^2 \rangle$ between the limits of $t=0$ (static holes) and $t \gg J$ in the one- and two-hole subspaces, respectively. In other words, if instead of $\chi_{\rm pl}$ we would consider $\bar{\chi}_{\rm pl} \approx \chi_{\rm pl} - C(0,0)$ we would obtain a result qualitatively similar to Fig. 17(a), i.e., $\bar{\chi}_{\rm pl}$ decreasing when t/J or x are increased. This result, together with similar conclusions for the frustrated Heisenberg model,[72] shows that there are no numerical indications that frustration (explicit or by holes) favors the uniform chiral state in simple models of high-T_c superconductivity.

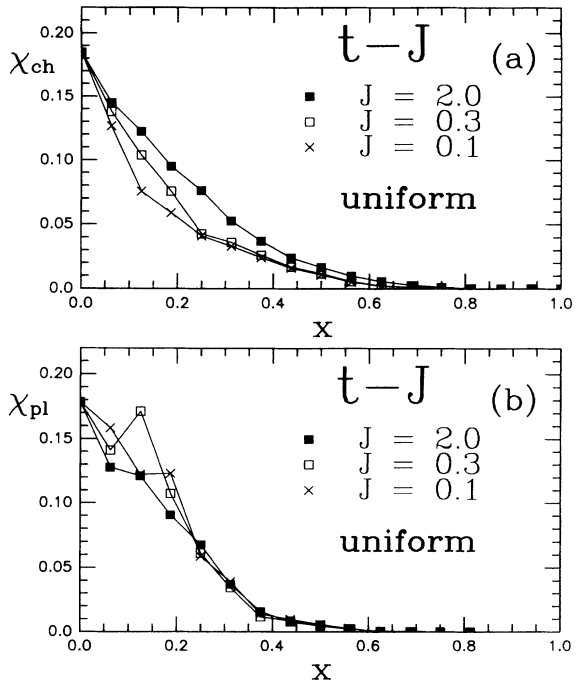

FIG. 17. (a) Uniform chiral correlation $\chi_{\rm ch}$ vs x (doping) at different values of J ($t=1$); (b) uniform chiral correlation $\chi_{\rm pl}$ vs x (doping) at different values of J ($t=1$).

However, the situation is not clear for *staggered* chiral order. Recently, some mean-field calculations[73] have shown that while the uniform chiral state is suppressed decreasing J/t, the corresponding staggered state is enhanced. To analyze this possible order we generalized the chiral and plaquette correlations to a finite momentum $\mathbf{q} = (\pi,\pi)$, by defining

$$\chi_{\rm pl}(\pi,\pi) = \left\langle \frac{1}{N} \left[\sum_{\mathbf{i}} (-1)^{\mathbf{i}_x + \mathbf{i}_y} O_{\mathbf{i}} \right]^2 \right\rangle$$

[$\chi_{\rm ch}(\pi,\pi)$ is analogously defined]. In Figs. 18(a) and 18(b) we present $\chi_{\rm ch}(\pi,\pi)$ and $\chi_{\rm pl}(\pi,\pi)$ vs x for different values of J/t. In the case of $\chi_{\rm ch}(\pi,\pi)$ the results are almost independent of J/t, which is qualitatively different behavior from that observed for the uniform case. At fixed J/t the correlations are still suppressed by doping. However, for $\chi_{\rm pl}(\pi,\pi)$ there is an *enhancement* with doping having a maximum near $x \sim 0.12$. At half filling a near cancellation in $\chi_{\rm pl}(\pi,\pi)$ between correlations at distance 0 and 1 strongly suppresses $\chi_{\rm pl}(\pi,\pi)$. This effect disappears with doping due to the previously mentioned increase of $C_{\rm pl}(0,0)$. $\chi_{\rm pl}(\pi,\pi)$ increases when J/t is reduced in agreement with the mean-field predictions and

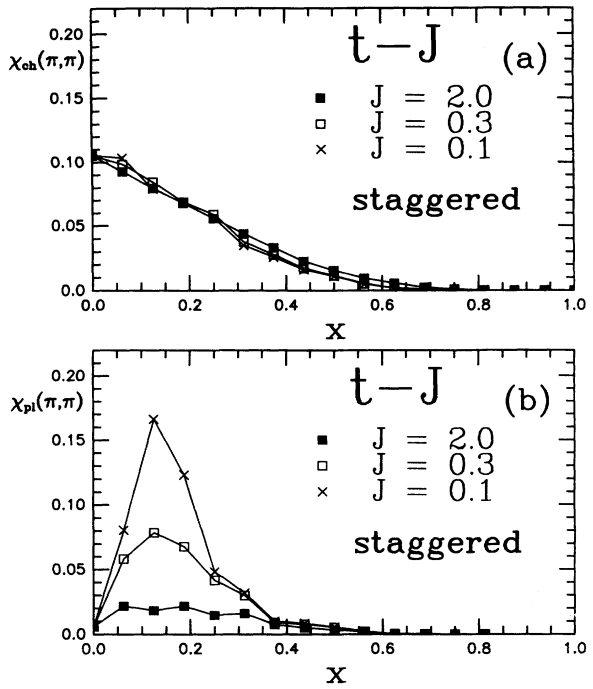

FIG. 18. (a) Staggered chiral correlation $\chi_{ch}(\pi,\pi)$ vs x (doping) at different values of J ($t=1$). (b) Staggered chiral correlation $\chi_{pl}(\pi,\pi)$ vs x (doping) at different values of J ($t=1$).

in contrast to the uniform case. Of course, the existence of staggered chiral LRO is difficult to analyze. Studying the correlation function $C_{pl}(\mathbf{i},\mathbf{j})$ we found that at a distance of one lattice spacing the plaquette correlations are mostly "ferromagnetic." However, at a distance $\sqrt{5}$ and realistic values of J/t, they become "antiferromagnetic," although very small in absolute value.[74,75]

X. SEARCHING FOR SPIRAL ORDER

Finally, we have also studied the possible existence of a "spiral" phase. It has been argued[76] that mobile holes induce a dipole distortion of the spins. Then, the spins are effectively ordered in an incommensurate (IC) pattern and to study this order we define the vector operator

$$\mathbf{T}_i=\mathbf{S}_i\times(\mathbf{S}_{i+x}+\mathbf{S}_{i+y}) , \tag{19}$$

and its associated correlation $\chi_{spi}=\langle(1/N)(\sum_i \mathbf{T}_i)^2\rangle$. The spin structure factor $S(\mathbf{q})$ was previously studied[17] finding that when doping is introduced in the t-J and Hubbard models, the AF peak at (π,π) decrease its intensity and moves towards $(0,\pi),(\pi,0)$, at least for small values of U/t.[45,77] For large U/t the splitting was also observed although it is not clear if it is along the diagonal in momentum space or towards $(0,\pi),(\pi,0)$. However, the intensity of this peak is small and there were no signs of divergence of the IC correlations. In Fig. 19 we present χ_{spi} vs x, showing that at small J/t and $x\sim 0.12$ there is an *enhancement* of the spiral order of about 25% with respect to half filling. This is the region where the shift in the AF peak with doping was found.[17]

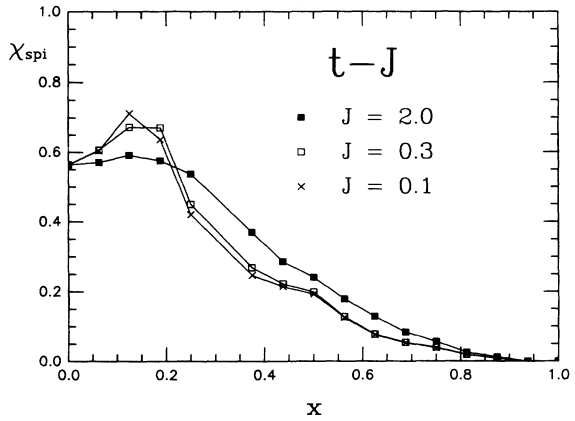

FIG. 19. Spiral correlation function χ_{spi} vs x (doping) at different values of J ($t=1$).

XI. CONCLUSIONS

In this paper we have presented a numerical study of the Hubbard and t-J models in two dimensions at all doping fractions. We have used exact diagonalization techniques on clusters of $\sqrt{10}\times\sqrt{10}$ and 4×4 sites and QMC simulations. We found that many of the features observed experimentally in the high-T_c compounds are qualitatively reproduced by models of strongly correlated electrons. In particular, we found that only a tiny fraction of holes is enough to destroy antiferromagnetic long-range order (although short-distance correlations remain important up to large dopings). This is due to the fact that a "dressed" hole has a finite size that increases as $J\to 0$ in the t-J model. Regarding the electronic density of states, $N(\omega)$, we observed that the chemical potential moves across the antiferromagnetic gap when holes or electrons are added to a half-filled system. In addition, new states appear in the gap and they fill it completely when U is smaller than or comparable to the bandwidth $8t$. These results are in agreement with x-ray absorption experiments[34] but not with photoemission experiments,[31] where the chemical potential was found to remain constant regardless of whether the doping is produced by holes or electrons. We have also analyzed in detail the optical conductivity, $\sigma_1(\omega)$, of the Hubbard and t-J models, finding many features in qualitative agreement with experiments. In particular, we found that the Drude peak increases its weight with doping (at small doping) and a mid-infrared band exists as observed experimentally. Another encouraging result that we observed numerically is the absence of indications of phase separation in the Hubbard model.

With respect to the possibility of superconductivity in these models our conclusions are the following: d-wave pairing correlations are enhanced near half filling where there are strong AF correlations. The extended s-wave equal-time pairing correlation is enhanced between half filling and 40% doping. However, we believe these results are mostly related to short-distance effects rather than with a genuine LRO in the superconducting operator. We based this conclusion in the study of the pairing correlations as a function of distance. If superconductivi-

ty actually exists in this model then $\langle \Delta \rangle$ is very small (the critical temperature would also be small) and its numerical analysis would be difficult even for larger lattices or using QMC methods.

What about more exotic forms of spin order? We did not observe evidence of *uniform* chiral order in this model. Correlations associated with triangle and plaquette operators do not show enhancement with doping. On the other hand, *staggered* chiral order seems enhanced by dynamical holes. However, we can show numerically that if the order parameter $\langle O \rangle$ is nonzero then it has to be very small. Finally, there is a tendency to spiral order at small J/t (i.e., $\sim 0.1-0.3$) and doping about 10–20%, which seems to be of short range.

Summarizing, our extensive numerical studies of the Hubbard and t-J models have shown that many features of the normal state of the superconducting cuprates considered anomalous have a natural explanation within these models. The electronic density of states, optical conductivity, and behavior of antiferromagnetism with doping are qualitatively reproduced by our small cluster results. On the other hand, a robust signal of superconductivity is still missing in these calculations. Although there is enhancement in particular pairing channels, it seems to arise mainly from short-distance effects.

Thus, we believe that there are two main directions for further work in the Hubbard model. The first one is to improve the pairing operators used in the numerical search for superconductivity. It has been argued[67] that it is necessary to consider extended quasiparticle operators rather than the standard fermionic operators to observe a susceptibility diverging with the volume. A second possibility is to modify the Hubbard model by the addition of phonons or longer-range interactions such that the short-distance properties tested by photoemission and optical conductivity remain but the long-distance behavior is changed to a possible superconducting regime. Work is in progress along both lines.

ACKNOWLEDGMENTS

We would like to acknowledge useful discussions with J. Allen, E. Gagliano, A. Kampf, R. Laughlin, and J.R. Schrieffer. This project was supported by NSF Grant Nos. PHY89-04035 and DMR90-02492, and the Electric Power Research Institute. The ESPRIT program P3041-MESH is also acknowledged for partial support. J. R. is supported by CONICET, Argentina. The computer calculations were done on the Cray-2 supercomputer at the National Center for Supercomputing Applications (NCSA), Urbana, Illinois. We thank NCSA for their support.

---

*Present address: Dipartimento di Fisica, Instituto Nazionale di Fisica Nucleare, Università di Bologna, via Irnerio 46, I-40126 Bologna, Italy.

†Present address: Physique des Solides, Univ. Paris–Sud, Bâtiment 510, 91405 Orsay CEDEX, France.

‡Present address: Departamento de Física, Facultad de Ciencias Exactas, Av. Pellegrini 250, 2000 Rosario, Argentina.

[1]J. G. Bednorz and K. A. Müller, Z. Phys. B **64**, 188 (1986); C. W. Chu *et al.*, Phys. Rev. Lett. **58**, 405 (1987).

[2]J. Zaanen, G. A. Sawatzky, and J. W. Allen, Phys. Rev. Lett. **55**, 418 (1985).

[3]$U/t = 8-12$ reproduces the phenomenology of the new materials ($J/t = 0.3-0.5$ in the t-J model). See, M. Schluter and M. Hybertsen, Physica C **162-164**, 583 (1989); M. Hybertsen, *et al.*, Phys. Rev. B **41**, 11 068 (1990); S. Bacci, E. Gagliano, R. Martin, and J. Annet, *ibid.* **44**, 7504 (1991).

[4]F. C. Zhang and T. M. Rice, Phys. Rev. B **37**, 3759 (1988).

[5]For a recent review, see E. Dagotto, Int. J. Mod. Phys. B **5**, 77 (1991).

[6]For a review of the method to obtain dynamical properties using a Lanczos algorithm, see E. Gagliano and C. Balseiro, Phys. Rev. Lett. **59**, 2999 (1987); and Ref. 5.

[7]For details on the diagonalization of the 4×4 cluster, see G. Fano, F. Ortolani, and F. Semeria, Int. J. Mod. Phys. B **3**, 1845 (1990).

[8]E. Dagotto, R. Joynt, A. Moreo, E. Gagliano, and S. Bacci, Phys. Rev. B **41**, 9049 (1990), and references therein.

[9]T. Barnes, A. Jacobs, M. Kovarik, and W. Macready, Phys. Rev. B **45**, 256 (1992).

[10]A state with these quantum numbers can be created from the ground state of eight electrons by acting with a pairing operator that destroys holes along the *diagonals* of the plaquettes having d-wave symmetry ["extended" d wave in the notation of A. Moreo and D. Scalapino, Phys. Rev. B **43**, 8211 (1991)].

[11]Recently, an s-wave enhancement in the pairing correlations was observed in the t-J model with four holes by J. Bonča, P. Prelovšek, and I. Sega, Solid State Commun. **78**, 109 (1991).

[12]Y. J. Uemura, J. Appl. Phys. **64**, 6087 (1988); Y. J. Uemura *et al.*, Physica C **162-164**, 857 (1989).

[13]G. Luke *et al.*, Phys. Rev. B **42**, 7981 (1990).

[14]H. Chou *et al.*, Phys. Rev. B **43**, 5554 (1991); P. Bourges *et al.*, *ibid.* **43**, 8690 (1991).

[15]The first excited state appearing in the spectral function Eq. (3) is not necessarily the first triplet with momentum $\mathbf{q}$ in the spectrum. However, Eq. (3) is very important since it is directly comparable with NMR experiments.

[16]In the other limit of low electronic density $x \sim 1$, the first excited state has also $\mathbf{q}=(\pi/2,\pi/2)$ and the energies are approximately J independent since the exchange term is inoperative (the probability of finding two spins at the same link is small). The fact that the state with $\mathbf{q}=(\pi/2,\pi/2)$ has such a low energy is compatible with a picture of free electrons ($U=0$) on a 4×4 lattice. In this limit considering, e.g., four particles, the ground state is formed by adding two particles to the $\mathbf{q}=(0,0)$ state, which has an energy (E) of -4 and the other two, to the states $\mathbf{q}=(0,\pi/2)$ plus its $(\pi/2)$-rotated ones, which have $E=-2$. To obtain a triplet excitation just flip one spin of those having energy -2. That introduces no additional cost in energy and it changes the momentum to $\mathbf{q}=(\pi/2,\pi/2)$ (note that in this result the size of the lattice is very important, and thus we expect strong finite-size effects at low concentration of electrons). Note that this result does not necessarily imply that $S(\mathbf{q})$ will move with doping away from $\mathbf{q}=(\pi,\pi)$ towards $\mathbf{q}=(\pi/2,\pi/2)$. For the t-J model the direction of movement of the split peak is ambiguous on a 4×4 lattice (Ref. 17).

[17]E. Moreo, A. Dagotto, T. Jolicoeur, and J. Riera, Phys. Rev. B **42**, 6222 (1990). See also A. Moreo *et al.*, *ibid.* **41**, 2313 (1990).

[18]E. Dagotto, A. Moreo and T. Barnes, Phys. Rev. B **40**, 6721 (1989).

[19]These ideas are similar to those of the spin-bag approach by A. Kampf and J. R. Schrieffer, Phys. Rev. B **42**, 7967 (1990).

[20]B. Shraiman and E. Siggia, Phys. Rev. Lett. **60**, 740 (1988).

[21]Recently, it has been claimed that x_c may be zero in the 2D Hubbard model [M. Furukawa and M. Imada (unpublished)] with a spin-spin correlation length varying as $1/\sqrt{x}$. This would imply that long-range order immediately disappears with doping rather than surviving till a small but finite critical concentration is reached, as discussed in the present paper. Only studies in large lattices will clarify this issue.

[22]This effect can be certainly alleviated by adding to the Hamiltonian an explicit Coulombic repulsion between holes (which has not been taken into account in the present study).

[23]V. Emery, S. Kivelson, and H. Lin, Phys. Rev. Lett. **64**, 475 (1990).

[24]A. Moreo, D. Scalapino, and E. Dagotto, Phys. Rev. B **43**, 11 442 (1991).

[25]J. Riera and A. P. Young, Phys. Rev. B **39**, 9697 (1989).

[26]G. Fano, F. Ortolani, and A. Parola, Phys. Rev. B **42**, 6877 (1990); and (unpublished). The binding energy in the Hubbard model was also evaluated using QMC methods by E. Dagotto, A. Moreo, R. Sugar, and D. Toussaint, Phys. Rev. B **41**, 811 (1990).

[27]Of course, discontinuities in the density vs chemical potential curves of size smaller than $\frac{1}{16}$ cannot be observed in our small lattice and thus our results actually put upper bounds to the difference of density in the two phases if phase separation would occur.

[28]M. Ogata, M. Luchini, S. Sorella, and F. Assad, Phys. Rev. Lett. **66**, 2388 (1991).

[29]In Kong-Ju-Bock and P. Schlottman, Phys. Rev. B **40**, 9104 (1989); F. Woynarovich, *ibid.* **43**, 11 448 (1991); P. Schlottman, *ibid.* **43**, 11 451 (1991); the behavior of the magnetization of the 1D negative-U Hubbard model as a function of an external magnetic field was discussed. By a particle-hole transformation those results can be easily mapped into the positive-U model with a chemical potential.

[30]W. Putikka, M. Luchini, and T. M. Rice, Phys. Rev. Lett. **68**, 538 (1992).

[31]J. W. Allen *et al.*, Phys. Rev. Lett. **64**, 595 (1990).

[32]J. Fink *et al.* (unpublished); Z.-X. Shen, *et al.*, Phys. Rev. B **36**, 8414 (1987); T. Takahashi *et al.*, Physica C **170**, 416 (1990); H. Matsuyama *et al.*, *ibid.* **160**, 567 (1989).

[33]T. Takahashi *et al.* (unpublished).

[34]C. T. Chen *et al.*, Phys. Rev. Lett. **66**, 104 (1991). See also H. Romberg *et al.*, Phys. Rev. B **42**, 8768 (1990).

[35]M. Alexander *et al.*, Phys. Rev. B **43**, 333 (1991).

[36]A shorter version of this section was presented by E. Dagotto, A. Moreo, F. Ortolani, J. Riera, and D. Scalapino, Phys. Rev. Lett. **67**, 1918 (1991).

[37]Similar results have been obtained for an eight-site cluster by T. Tohyama and S. Maekawa (private communication).

[38]G. A. Sawatzky (unpublished).

[39]H. Eskes and G. Sawatzky, Phys. Rev. B **43**, 119 (1991); C. Sá de Melo and S. Doniach, *ibid.* **41**, 6633 (1990); R. Scalettar *et al.* (unpublished).

[40]See also J. R. Schrieffer and A. Kampf, Proceedings of the Workshop on Fermiology of High-T_c Superconductors [J. Phys. Chem. Solids (to be published)]; A. Kampf and J. R. Schrieffer (unpublished).

[41]Results for two holes in the t-J model have been presented by W. Stephan and P. Horsch, Phys. Rev. Lett. **66**, 2258 (1991).

[42]G. A. Thomas *et al.*, Phys. Rev. Lett. **61**, 1313 (1988); T. Timusk *et al.*, Phys. Rev. B **38**, 6683 (1988); R. T. Collins *et al.*, *ibid.* **39**, 6571 (1989); S. L. Cooper *et al.*, *ibid.* **40**, 11 358 (1989); Z. Schlesinger *et al.*, *ibid.* **41**, 11 237 (1990); J. Orenstein *et al.*, *ibid.* **42**, 6342 (1990); Ji-Guang Zhang *et al.*, *ibid.* **43**, 5389 (1991); R. Collins, *et al.*, *ibid.* **43**, 8701 (1991).

[43]S. L. Cooper *et al.*, Phys. Rev. B **41**, 11 605 (1990); J. Orenstein *et al.*, *ibid.* **42**, 6342 (1990).

[44]S. Uchida *et al.*, Phys. Rev. B **43**, 7942 (1991).

[45]A. Moreo *et al.*, Phys. Rev. B **41**, 2313 (1990).

[46]A previous study of $\sigma_1(\omega)$ in the 2D Hubbard model on finite clusters was reported by A. Moreo and E. Dagotto, Phys. Rev. B **42**, 4786 (1990) for a $\sqrt{10}\times\sqrt{10}$ site lattice with open boundary conditions.

[47]A shorter version of this section was presented by E. Dagotto, A. Moreo, F. Ortolani, J. Riera, and D. Scalapino (unpublished).

[48]P. F. Maldague, Phys. Rev. B **16**, 2437 (1977).

[49]W. Kohn, Phys. Rev. **133**, A171 (1964).

[50]B. Shastry and B. Sutherland, Phys. Rev. Lett. **65**, 243 (1990).

[51]R. M. Fye, M. Martins, D. Scalapino, J. Wagner, and W. Hanke (unpublished). See also J. Wagner, W. Hanke, and D. Scalapino, Phys. Rev. B **43**, 10 517 (1991); C. Stafford, A. Millis, and B. Shastry, *ibid.* **43**, 13 660 (1991). The absence of spectral weight in $\sigma_1(\omega)$ between the Drude peak and the charge excitations bands in the 1D Hubbard model has been shown using the Bethe ansatz by J. Carmelo (private communication).

[52]In T. Tohyama and S. Maekawa, J. Phys. Soc. J. (to be published), a 1D Cu-O cluster was studied.

[53]On the 4×4 cluster we observed important finite-size effects (FSE's) working with 14 electrons ($x=0.125$). In this case and at small U/t, the current operator connects the ground state with another state of energy order U/t (that becomes degenerate with the ground state at $U/t=0$) with a matrix element of order 1. Then, its contribution to $\sigma_1(\omega)$ diverges as $U/t\rightarrow0$ and the Drude peak $\rightarrow-\infty$. This is similar to the results observed in Ref. 51 at half filling and it is a FSE that will disappear in the bulk limit. We have simply subtracted this anomalous peak at low energies (located at $\omega=0.463$ at $U/t=10$ and 14 electrons) from our Fig. 11(b) and in the calculation of D_n [Fig. 12(b)]. We found that this procedure produces results which smoothly connect with those of other dopings. Another approach would have been to use twisted boundary conditions [D. Poilblanc and E. Dagotto (unpublished); D. Poilbanc (unpublished)] but such a calculation would have been very difficult for the 4×4 Hubbard cluster.

[54]Note that *independent* calculations (Ref. 3) done by comparing the spectrum of the three- and one-band models have obtained similar values for U/t.

[55]However, notice that D becomes negative at half filling. This is indeed a finite-size effect. As previously reported [Ref. 51; A. Moreo (unpublished); and C. Stafford, A. Millis, and B. Shastry, Phys. Rev. B **43**, 13 660 (1991)], for a half-filled finite system, D can be negative, indicating a paramagnetic response. For the 1D ring, this reponse was found to decrease as $\exp(-N_x/\xi)$, and we expect that this same behavior will be seen for two-dimensional clusters. Actually, at half filling, the Drude weight is a small number coming out from the cancellation of two large numbers [Eq. (13)] and thus it is not

surprising that D near half filling is subject to important finite-size effects. Regretfully there are no other numerical methods rather than Lanczos methods to reliably study the optical conductivity.

[56]Previous work on the t-J model has been reported by T. M. Rice and F. C. Zhang, Phys. Rev. B **39**, 815 (1989); I. Sega and P. Prelovšek, *ibid.* **42**, 892 (1990); A. Moreo and E. Dagotto, *ibid.* **42**, 4786 (1990); W. Stephan and P. Horsch, *ibid.* **42**, 8736 (1990); C.-X. Chen and H.-B. Schüttler, *ibid.* **43**, 3771 (1991); J. Inoue and S. Maekawa, J. Phys. Soc. Jpn. **59**, 2110 (1990); A. Millis and S. Coppersmith, Phys. Rev. B **42**, 10 807 (1990).

[57]W. Stephan (private communication).

[58]These numbers are in good agreement with recent variational calculations using the Kalmeyer-Laughlin spin-liquid state [R. Laughlin (private communication)].

[59]The behavior of the positive-U model can be contrasted with the negative-U case, which has a finite Drude weight even at half-filling, low-lying spectral weight inside the gap, and whose distribution of spectral weight does not vary rapidly as the system is initially doped away from half-filling (Ref. 47).

[60]If at a given x the ground state is degenerate, then the correlations are averaged over that degeneracy. We follow this convention for all the results in Secs. VIII–X.

[61]A. Moreo and D. Scalapino, Phys. Rev. B **43**, 8211 (1991).

[62]However, recently [E. Dagotto *et al.*, Phys. Rev. B **42**, 2347 (1990)] it has been observed that the s- and d-wave *dynamical* pairing correlation functions are drastically different in the two-hole subspace: the d wave has spectral weight at small ω while the s-wave spectral weight is mainly concentrated at large ω.

[63]K. Miyake *et al.*, Phys. Rev. B **34**, 6554 (1986); D. Scalapino *et al.*, *ibid.* **34**, 8190 (1986); C. Gros, *ibid.* **38**, 931 (1988).

[64]A. Moreo (unpublished).

[65]Recent studies in the three-band Hubbard model [G. Dopf *et al.*, Phys. Rev. B **41**, 9264 (1990); M. Frick *et al.*, *ibid.* **42**, 2665 (1990)] have obtained similar results, i.e., enhancement of s-wave correlations but no LRO. For the one-band Hubbard model see also J. Hirsch and S. Tang, Phys. Rev. Lett. **62**, 591 (1989); M. Imada, J. Phys. Soc. Jpn. **57**, 42 (1988).

[66]M. Imada (unpublished).

[67]E. Dagotto and J. R. Schrieffer, Phys. Rev. B **43**, 8705 (1991).

[68]I. Affleck and J. Marston, Phys. Rev. B **37**, 3774 (1988); P. W. Anderson *et al.*, *ibid.* **40**, 8939 (1989).

[69]Three of us recently reported results for two holes in the t-J model including the dynamical response of operators related with chiral order. See D. Poilblanc, E. Dagotto, and J. Riera, Phys. Rev. B **43**, 7899 (1991).

[70]P. A. Lee (unpublished).

[71]P. Lederer, D. Poilblanc, and T. M. Rice, Phys. Rev. Lett. **63**, 1519 (1989); D. Poilblanc *et al.*, Phys. Rev. B **41**, 1949 (1990); D. Poilblanc, *ibid.* **41**, 4827 (1990).

[72]E. Dagotto and A. Moreo, Phys. Rev. Lett. **63**, 2148 (1989). See also M. Imada (unpublished).

[73]D. Poilblanc and Y. Hasegawa, Phys. Rev. B **41**, 6989 (1990).

[74]The energy gap of the staggered chiral operator goes from $\sim 6J$ for zero hole to $\sim 2.5J$ with two holes. This result is almost t independent, although the spectral weight at low energies grows with decreasing J/t. At the same time the spin-wave energy changes from $0.6J$ at half filling to $0.75J$ with two holes at $J/t=0.3$.

[75]It is possible to put a bound on $\langle O \rangle$ by considering the plaquette-plaquette correlation function: for example, at $J/t=0.15$ and distance $2\sqrt{2}$ the correlation produces a bound $|\langle O \rangle| < 0.04$. Although this number seems very small, in a recent variational Monte Carlo calculation of the uniform flux phase [M. Ogata and T. M. Rice (unpublished)] a result similar in magnitude has been found ($\langle O \rangle \sim 0.12$) and thus we cannot completely exclude the existence of LRO for chiral order. Our numerical results show that if $\langle O \rangle$ is nonzero, then it is very small.

[76]B. Shraiman and E. Siggia, Phys. Rev. Lett. **62**, 1564 (1989); C. Jayaprakash *et al.*, Phys. Rev. B **40**, 2610 (1989); C. Kane *et al.*, *ibid.* **41**, 2653 (1990).

[77]This result has been recently also found experimentally, S-W Cheong *et al.* (unpublished).